Table of Contents

Experimental section

Analytical Data

CHN Analysis: Carbon, hydrogen, and nitrogen elemental analyses were performed using a Thermo Scientific Flash EA – 1112. The polymers were placed in a tin crucible with no less than one mass equivalent to V_2O_5. The samples were prepared and stored under inert conditions until the time of measurements.

Vibrational Spectroscopy: ALPHA FT-IR spectrometer from Bruker optics (ATR module) using OPUS software was used to record MIR spectra from several milligrams of the compounds.

Crystallographic Data

CCDC 2237763 (**4-Eu^{2+}**), 2237764 (**4-$^2_\infty$Tm**), 2237765 (**4-Yb**), 2237766 (**4-Lu**), 2237767 (**4-La**), 2237768 (**4-Ce**), 2237769 (**4-Pr**), 2237770 (**4-Nd**), 2237771 (**4-Ho**), 2237772 (**4-Er**), 2237773 (**3-Ce**), 2237774 (**3-Pr**), 2237775 (**3-Nd**), 2237776 (**3-Ho**), 2237777 (**3-Er**), and 2237778 (**3-Tm**) contain the supplementary crystallographic data. These data are provided free of charge by the Cambridge Crystallographic Data Centre.

Table S1. Crystallographic data of $^2_\infty$[Eu(4-PyPz)$_2$(Py)$_2$] (**4-Eu^{2+}**) and $^2_\infty$[Ln$_2$(4-PyPzH)$_6$]·Py, Ln = Yb (**4-Yb**) and Lu (**4-Lu**).

Compound	**$^2_\infty$[Eu(4-PyPz)$_2$(Py)$_2$]**	**$^2_\infty$[Yb$_2$(4-PyPzH)$_6$]·Py**	**$^2_\infty$[Lu$_2$(4-PyPzH)$_6$]·Py**
CCDC number	2237763	2237765	2237766
Empirical formula	$C_{26}H_{22}N_8Eu$	$C_{53}H_{41}N_{19}Yb_2$	$C_{53}H_{41}N_{19}Lu_2$
M_r / g·mol^{-1}	598.47	1290.13	1293.99
T / K	100(2)	100(2)	100(2)
λ / pm	71.073, Mo-K$_\alpha$	71.073, Mo-K$_\alpha$	71.073 Mo-K$_\alpha$
Crystal system	Monoclinic	Monoclinic	Monoclinic
Space group	$P2_1$	$P2_1/n$	$P2_1/n$
a / pm	944.4(1)	1701.5(2)	1702.1(2)
b / pm	1458.4(1)	910.7(1)	909.5(1)
c / pm	997.6(1)	3161.8(4)	3155.2(4)
α, γ / °	90	90	90
β / °	117.170(4)	97.289(5)	97.109(4)
V / 10^6 pm^3	1222.4(2)	4859(1)	4846.9(9)
Z	2	4	4
ρ_{calc} / g·cm^{-3}	1.626	1.763	1.773
μ / mm^{-1}	2.596	3.886	4.110
F(000)	594	2528	2536
Crystal size / mm^3	0.070 x 0.060 x 0.030	0.129 x 0.079 x 0.050	0.204 x 0.039 x 0.018
θ_{min} / °	2.295	2.157	2.163
θ_{max} / °	27.567	27.577	27.635
Reflections collected	44595	154420	164975
Independent reflections	5603	11219	11219
R(int)	0.0414	0.1890	0.1214
No. Of parameters	316	810	810
GOF	1.137	1.066	1.047
Final R indices [$I > 2\sigma$(I)]	R_1 = 0.0141, wR_2 = 0.0296	R_1 = 0.0515, wR_2 = 0.0849	R_1 = 0.0404, wR_2 = 0.0835
R indices (all data)	R_1 = 0.0159, wR_2 = 0.0302	R_1 = 0.1120, wR_2 = 0.1022	R_1 = 0.0734, wR_2 = 0.0962
$\Delta\rho_{max}$, $\Delta\rho_{min}$ / e·10^{-6}·pm^{-3}	0.734, −0.619	2.364, −1.425	2.721, −2.064

Table S2. Crystallographic data of $^{2}_{\infty}$[Tm(4-PyPz)$_3$(Py)] (**4-$^{2}_{\infty}$Tm**).

Compound	**$^{2}_{\infty}$[Tm(4-PyPz)$_3$(Py)]**
CCDC number	2237764
Empirical formula	$C_{29}H_{23}N_{10}Tm$
M_r / g·mol^{-1}	680.50
T / K	100(2)
λ / pm	71.073, Mo-K$_\alpha$
Crystal system	Monoclinic
Space group	*Cc*
a / pm	1028.4(1)
b / pm	1507.8(1)
c / pm	1753.0(2)
α, γ / °	90
β / °	97.759(2)
V / 10^6 pm^3	2693.2(4)
Z	4
ρ_{calc} / g·cm^{-3}	1.678
μ / mm^{-1}	3.333
F(000)	1344
Crystal size / mm^3	0.055 x 0.023 x 0.020
θ_{min} / °	2.345
θ_{max} / °	27.160
Reflections collected	42246
Independent reflections	5807
R(int)	0.0860
Flack x	0.003(7)
No. Of parameters	361
GOF	1.039
Final *R* indices [$I > 2\sigma$(I)]	R_1 = 0.0286, wR_2 = 0.0472
R indices (all data)	R_1 = 0.0387, wR_2 = 0.0494
$\Delta\rho_{max}$, $\Delta\rho_{min}$ / e·10^{-6}·pm^{-3}	1.628, −0.744

Table S3. Crystallographic data of $^{3}_{\infty}$[Ln(4-PyPz)$_3$], Ln = La (**4-La**), Ce (**4-Ce**), Pr (**4-Pr**), and Nd (**4-Nd**).

Compound	**$^{3}_{\infty}$[La(4-PyPz)$_3$]**	**$^{3}_{\infty}$[Ce(4-PyPz)$_3$]**	**$^{3}_{\infty}$[Pr(4-PyPz)$_3$]**	**$^{3}_{\infty}$[Nd(4-PyPz)$_3$]**
CCDC number	2237767	2237768	2237769	2237770
Empirical formula	$C_{24}H_{18}N_9La$	$C_{24}H_{18}N_9Ce$	$C_{24}H_{18}N_9Pr$	$C_{24}H_{18}N_9Nd$
M_r / g·mol^{-1}	571.38	572.59	573.38	576.71
T / K	100(2)	100(2)	100(2)	100(2)
λ / pm	0.71073	0.71073	0.71073	0.71073
Crystal system	Monoclinic	Monoclinic	Monoclinic	Monoclinic
Space group	$P2_1/n$	$P2_1/n$	$P2_1/n$	$P2_1/n$
a / pm	934.0(2)	929.4(1)	927.9(2)	928.1(1)
b / pm	1693.2(3)	1689.7(1)	1687.5(2)	1689.6(2)
c / pm	1598.9(3)	1593.1(1)	1589.8(2)	1585.4(2)
α, γ / °	90	90	90	90
β / °	102.364(6)	102.384(2)	102.351(5)	102.289(4)
V / 10^6 pm^3	2469.9(7)	2443.6(2)	2431.5(6)	2429.1(4)
Z	4	4	4	4
ρ_{calc} / g·cm^{-3}	1.537	1.556	1.566	1.577
μ / mm^{-1}	1.759	1.893	2.034	2.168
F(000)	1128	1132	1136	1140
Crystal size / mm^3	0.026 x 0.013 x 0.010	0.042 x 0.021 x 0.017	0.055 x 0.022 x 0.015	0.789 x 0.147 x 0.075
θ_{min} / °	2.332	1.779	2.347	1.783
θ_{max} / °	26.501	27.103	27.533	27.485
Reflections collected	61095	85383	97993	61076
Independent reflections	5114	5395	5589	5565
R(int)	0.1635	0.1290	0.0941	0.0480
No. Of parameters	307	307	307	307
GOF	1.028	1.031	1.048	1.118
Final R indices [$I > 2\sigma$(I)]	R_1 = 0.0365, wR_2 = 0.0715	R_1 = 0.0290, wR_2 = 0.0530	R_1 = 0.0271, wR_2 = 0.0525	R_1 = 0.0225, wR_2 = 0.0509
R indices (all data)	R_1 = 0.0665, wR_2 = 0.0804	R_1 = 0.0491, wR_2 = 0.0585	R_1 = 0.0408, wR_2 = 0.0572	R_1 = 0.0276, wR_2 = 0.0528
$\Delta\rho_{max}$, $\Delta\rho_{min}$ / e·10^{-6}·pm^{-3}	1.611, −0.631	1.579, −0.661	1.651, −0.651	1.424, −0.898

Table S4. Crystallographic data of $^{3}_{\infty}$[Ln(4-PyPz)$_3$], Ln = Ho (**4-Ho**) and Er (**4-Er**).

Compound	**$^{3}_{\infty}$[Ho(4-PyPz)$_3$]**	**$^{3}_{\infty}$[Er(4-PyPz)$_3$]**
CCDC number	2237771	2237772
Empirical formula	$C_{24}H_{18}N_9Ho$	$C_{24}H_{18}N_9Er$
M_r / g·mol^{-1}	597.40	599.73
T / K	100(2)	100(2)
λ / pm	0.71073	0.71073
Crystal system	Monoclinic	Monoclinic
Space group	$P2_1/n$	$P2_1/n$
a / pm	915.9(2)	913.4(1)
b / pm	1674.0(2)	1673.0(2)
c / pm	1571.4(2)	1565.9(2)
α, γ / °	90	90
β / °	102.280(6)	102.156(5)
V / 10^6 pm^3	2354.2(6)	2339.3(3)
Z	4	4
ρ_{calc} / g·cm^{-3}	1.686	1.703
μ / mm^{-1}	3.392	3.619
F(000)	1168	1172
Crystal size / mm^3	0.114 x 0.070 x 0.034	0.116 x 0.073 x 0.043
θ_{min} / °	1.800	1.803
θ_{max} / °	27.557	27.377
Reflections collected	5422	5252
Independent reflections	5422	5252
No. Of parameters	308	308
GOF	1.111	1.053
Final R indices [$I > 2\sigma(I)$]	R_1 = 0.0296, wR_2 = 0.0603	R_1 = 0.0305, wR_2 = 0.0617
R indices (all data)	R_1 = 0.0398, wR_2 = 0.0641	R_1 = 0.0443, wR_2 = 0.0659
$\Delta\rho_{max}$, $\Delta\rho_{min}$ / e·10^{-6}·pm^{-3}	2.670, −1.636	2.145, −1.695

Table S5. Crystallographic data of $^{3}_{\infty}$[Ln(3-PyPz)$_3$], Ln = Ce (**3-Ce**), Pr (**3-Pr**), Nd (**3-Nd**), and Ho (**3-Ho**).

Compound	**$^{3}_{\infty}$[Ce(3-PyPz)$_3$]**	**$^{3}_{\infty}$[Pr(3-PyPz)$_3$]**	**$^{3}_{\infty}$[Nd(3-PyPz)$_3$]**	**$^{3}_{\infty}$[Ho(3-PyPz)$_3$]**
CCDC number	2237773	2237774	2237775	2237776
Empirical formula	$C_{24}H_{18}N_9Ce$	$C_{24}H_{18}N_9Pr$	$C_{24}H_{18}N_9Nd$	$C_{24}H_{18}N_9Ho$
M_r / g·mol^{-1}	572.59	573.38	576.71	597.40
T / K	100(2)	100(2)	100(2)	100(2)
λ / pm	0.71073	0.71073	0.71073	0.71073
Crystal system	Cubic	Cubic	Cubic	Cubic
Space group	$Pa\bar{3}$	$Pa\bar{3}$	$Pa\bar{3}$	$Pa\bar{3}$
a, b, c / pm	1724.8(1)	1720.9(1)	1717.9(1)	1698.8(1)
α, β, γ / °	90	90	90	90
V / 10^6 pm^3	5131.2(7)	5096.1(4)	5069.8(3)	4902.3(4)
Z	8	8	8	8
ρ_{calc} / g·cm^{-3}	1.482	1.495	1.511	1.619
μ / mm^{-1}	1.803	1.941	2.077	3.258
F(000)	2264	2272	2280	2336
Crystal size / mm^3	0.105 x 0.094 x 0.075	0.086 x 0.052 x 0.043	0.059 x 0.041 x 0.018	0.138 x 0.094 x 0.065
θ_{min} / °	2.045	2.050	2.053	2.076
θ_{max} / °	27.074	26.718	27.522	27.524
Reflections collected	37796	48365	86496	97322
Independent reflections	1889	1815	1955	1888
R(int)	0.1778	0.0775	0.0990	0.0644
No. Of parameters	103	103	103	103
GOF	1.065	1.096	1.100	1.066
Final R indices [$I > 2\sigma$(I)]	R_1 = 0.0399, wR_2 = 0.0669	R_1 = 0.0248, wR_2 = 0.0493	R_1 = 0.0266, wR_2 = 0.0506	R_1 = 0.0221, wR_2 = 0.0487
R indices (all data)	R_1 = 0.0808, wR_2 = 0.0784	R_1 = 0.0382, wR_2 = 0.0535	R_1 = 0.0427, wR_2 = 0.0555	R_1 = 0.0297, wR_2 = 0.0517
$\Delta\rho_{max}$, $\Delta\rho_{min}$ / e·10^{-6}·pm^{-3}	1.325, −0.530	0.674, −0.567	0.843, −0.546	0.799, −0.641

Table S6. Crystallographic data of $^{3}_{\infty}$[Ln(3-PyPz)$_3$], Ln = Er (**3-Er**) and Tm (**3-Tm**).

Compound	**$^{3}_{\infty}$[Er(3-PyPz)$_3$]**	**$^{3}_{\infty}$[Tm(3-PyPz)$_3$]**
CCDC number	2237777	2237778
Empirical formula	$C_{24}H_{18}N_9Er$	$C_{24}H_{18}N_9Tm$
M_r / g·mol^{-1}	599.73	601.40
T / K	100(2)	100(2)
λ / pm	0.71073	0.71073
Crystal system	Cubic	Cubic
Space group	$Pa\bar{3}$	$Pa\bar{3}$
a, b, c / pm	1695.5(1)	1695.2(4)
α, β, γ / °	90	90
V / 10^6 pm^3	4874.2(3)	4872(3)
Z	8	8
ρ_{calc} / g·cm^{-3}	1.635	1.640
μ / mm^{-1}	3.474	3.672
F(000)	2344	2352
Crystal size / mm^3	0.093 x 0.089 x 0.074	0.051 x 0.027 x 0.012
θ_{min} / °	2.080	2.081
θ_{max} / °	27.520	25.701
Reflections collected	30024	39425
Independent reflections	1883	1558
R(int)	0.0670	0.1755
No. Of parameters	103	103
GOF	1.098	1.070
Final R indices [$I > 2\sigma(I)$]	R_1 = 0.0247, wR_2 = 0.0481	R_1 = 0.0386, wR_2 = 0.0718
R indices (all data)	R_1 = 0.0382, wR_2 = 0.0521	R_1 = 0.0715, wR_2 = 0.0824
$\Delta\rho_{max}$, $\Delta\rho_{min}$ / e·10^{-6}·pm^{-3}	1.160, −0.601	1.580, −0.905

Interatomic Distances and Angles

Table S7. Selected interatomic distances (pm) and angles (◦) of $^{2}_{\infty}$[Eu(4-PyPz)$_2$(Py)$_2$] (**4-Eu^{2+}**). Symmetry operations: I x+1,y,z II −x+1,y+1/2,−z.

Atoms	$^{2}_{\infty}$[Eu(4-PyPz)$_2$(Py)$_2$]	Atoms	$^{2}_{\infty}$[Eu(4-PyPz)$_2$(Py)$_2$]
Eu1-N1	270.0(2)	N3^{I}-Eu1-N4^{II}	157.2(1)
Eu1-N2^{I}	256.8(4)	N3^{I}-Eu1-N6	114.8(1)
Eu1-N3^{I}	264.1(2)	N3^{I}-Eu1-N7	116.0(1)
Eu1-N4^{II}	272.8(2)	N3^{I}-Eu1-N8	82.1(1)
Eu1-N5	254.9(4)	N4^{II}-Eu1-N8	79.8(1)
Eu1-N6	268.0(4)	N5-Eu1-N1	85.4(1)
Eu1-N7	272.3(4)	N5-Eu1-N2^{I}	90.4(1)
Eu1-N8	274.5(2)	N5-Eu1-N3^{I}	86.6(1)
N1-Eu1-N4^{II}	76.9(1)	N5-Eu1-N4^{II}	108.6(1)
N1-Eu1-N7	153.1(1)	N5-Eu1-N6	30.2(1)
N1-Eu1-N8	85.0(1)	N5-Eu1-N7	107.1(1)
N2^{I}-Eu1-N1	118.2(1)	N5-Eu1-N8	165.4(1)
N2^{I}-Eu1-N3^{I}	30.3(1)	N6-Eu1-N1	97.0(1)
N2^{I}-Eu1-N4^{II}	157.3(1)	N6-Eu1-N4^{II}	84.3(1)
N2^{I}-Eu1-N6	108.9(2)	N6-Eu1-N7	84.4(1)
N2^{I}-Eu1-N7	86.2(1)	N6-Eu1-N8	163.1(1)
N2^{I}-Eu1-N8	84.5(2)	N7-Eu1-N4^{II}	76.5(1)
N3^{I}-Eu1-N1	87.9(1)	N7-Eu1-N8	86.3(1)

Table S8. Selected interatomic distances (pm) and angles (◦) of $^{2}_{\infty}$[Ln$_2$(4-PyPzH)$_6$]·Py, Ln = Yb(**4-Yb**), Lu (**4-Lu**). Symmetry operations: I −x+1/2,y−1/2,−z+1/2 II x,y−1,z III −x+1/2,y−1/2,−z+3/2 IV x,y+1,z

Atoms	$^{2}_{\infty}$[Yb(4-PyPzH)$_6$]·Py	$^{2}_{\infty}$[Lu(4-PyPzH)$_6$]·Py	Atoms	$^{2}_{\infty}$[Yb(4-PyPzH)$_6$]·Py	$^{2}_{\infty}$[Lu(4-PyPzH)$_6$]·Py
Ln1-N7	245(2)	245(1)	N17-Ln1-N10^{II}	83.9(2)	84.2(2)
Ln1-N10^{II}	257.5(5)	256.7(4)	N17-Ln1-N12	160.4(2)	159.8(2)
Ln1-N11	234.1(6)	234.0(4)	N17-Ln1-N13^{I}	84.4(2)	84.3(2)
Ln1-N12	242.0(5)	240.2(5)	N17-Ln1-N14	80.3(2)	79.9(2)
Ln1-N13^{I}	247.5(5)	245.2(4)	N17-Ln1-N15	80.9(2)	80.4(2)
Ln1-N14	239.9(6)	239.2(4)	N18-Ln1-N7	78.5(4)	78.2(3)
Ln1-N15	238.2(6)	236.6(4)	N18-Ln1-N10^{II}	76.7(2)	76.5(2)
Ln1-N17	235.8(6)	235.1(4)	N18-Ln1-N12	148.0(2)	146.9(2)
Ln1-N18	234.1(6)	234.6(5)	N18-Ln1-N13^{I}	112.4(2)	113(2)
Ln2-N1^{IV}	247.9(6)	244.5(4)	N18-Ln1-N14	98.8(2)	99.2(2)
Ln2-N2	232.3(6)	232.6(4)	N18-Ln1-N15	82.1(2)	82.1(2)
Ln2-N3	231.0(6)	231.5(5)	N18-Ln1-N17	32.9(2)	33.9(2)
Ln2-N4^{III}	245.4(5)	243.5(4)	N2-Ln2-N1^{IV}	115.9(2)	116.5(2)
Ln2-N5	227.7(6)	228.0(4)	N2-Ln2-N4^{III}	85.3(2)	85.1(2)
Ln2-N6	231.2(6)	231.9(5)	N2-Ln2-N8	108.4(5)	109.4(3)
Ln2-N8	237(2)	236(1)	N2-Ln2-N9	137.6(3)	139.4(5)
Ln2-N9	241(2)	243(1)	N3-Ln2-N1^{IV}	83.1(2)	83.7(2)
N7-Ln1-N10^{II}	87.0(3)	86.7(3)	N3-Ln2-N2	34.3(2)	34.2(2)
N7-Ln1-N13^{I}	154.0(3)	153.5(2)	N3-Ln2-N4^{III}	116.8(2)	116.5(2)
N11-Ln1-N7	81.5(4)	80.9(3)	N3-Ln2-N6	105.0(2)	104.2(2)

N11-Ln1-N10^{II}	112.1(2)	112.4(2)	N3-Ln2-N8	92.8(5)	93.9(3)
N11-Ln1-N12	32.3(2)	33.4(2)	N3-Ln2-N9	125.7(4)	126.9(4)
N11-Ln1-N13^{I}	89.9(2)	90.2(2)	N4^{III}-Ln2-N1^{IV}	158.5(2)	158.0(2)
N11-Ln1-N14	81.1(2)	80.9(2)	N5-Ln2-N1^{IV}	86.8(2)	86.5(2)
N11-Ln1-N15	86.2(2)	86.0(2)	N5-Ln2-N2	125.8(2)	125.5(2)
N11-Ln1-N17	160.8(2)	160.3(2)	N5-Ln2-N3	138.1(2)	137.4(2)
N11-Ln1-N18	157.7(2)	156.8(2)	N5-Ln2-N4^{III}	83.1(2)	83.7(2)
N12-Ln1-N7	79.0(4)	78.5(3)	N5-Ln2-N6	34.8(2)	34.8(2)
N12-Ln1-N10^{II}	79.8(2)	79(2)	N5-Ln2-N8	124.7(4)	124.1(3)
N12-Ln1-N13^{I}	80.7(2)	80.5(2)	N5-Ln2-N9	92.2(4)	91.1(4)
N13^{I}-Ln1-N10^{II}	73.5(2)	73.7(2)	N6-Ln2-N1^{IV}	92.6(2)	92.2(2)
N14-Ln1-N7	115.8(3)	116.0(3)	N6-Ln2-N2	92.7(2)	92.5(2)
N14-Ln1-N10^{II}	155.7(2)	155.9(2)	N6-Ln2-N4^{III}	89.9(2)	90.9(2)
N14-Ln1-N12	111.3(2)	112.0(2)	N6-Ln2-N8	158.9(5)	158.1(4)
N14-Ln1-N13^{I}	86.7(2)	86.7(2)	N6-Ln2-N9	127.0(3)	125.9(4)
N15-Ln1-N7	84.1(3)	84.8(2)	N8-Ln2-N1^{IV}	78.1(5)	77.4(4)
N15-Ln1-N10^{II}	158.3(2)	158.2(2)	N8-Ln2-N4^{III}	92.1(5)	91.9(4)
N15-Ln1-N12	117.7(2)	118.7(2)	N8-Ln2-N9	33.2(4)	33.5(3)
N15-Ln1-N13^{I}	119.9(2)	119.7(2)	N9-Ln2-N1^{IV}	80.3(3)	78.5(5)
N15-Ln1-N14	33.5(2)	33.2(2)	N9-Ln2-N4^{III}	81.1(3)	82.0(5)
N17-Ln1-N7	111.0(4)	111.7(3)			

Table S9. Selected interatomic distances (pm) and angles (◦) of $^{2}_{\infty}$[Tm(4-PyPz)$_3$(Py)] (**4-$^{2}_{\infty}$Tm**). Symmetry operations: I x−1/2,y+1/2,z II x+1/2,y+1/2,z.

Atoms	**$^{2}_{\infty}$[Tm(4-PyPz)$_3$(Py)]**	**Atoms**	**$^{2}_{\infty}$[Tm(4-PyPz)$_3$(Py)]**
Tm1-N1^{II}	259.2(5)	N5-Tm1-N4^{I}	117.2(2)
Tm1-N2	234.5(5)	N5-Tm1-N10	85.3(2)
Tm1-N3	241.4(5)	N6-Tm1-N1^{II}	158.9(2)
Tm1-N4^{I}	246.5(5)	N6-Tm1-N3	117.6(2)
Tm1-N5	239.5(5)	N6-Tm1-N4^{I}	85.3(2)
Tm1-N6	234.9(5)	N6-Tm1-N5	33.5(2)
Tm1-N8	239.2(6)	N6-Tm1-N8	80.5(2)
Tm1-N9	232.4(6)	N6-Tm1-N10	118.4(2)
Tm1-N10	250.5(6)	N8-Tm1-N1^{II}	82.9(2)
N2-Tm1-N1^{II}	113.3(2)	N8-Tm1-N3	161.2(2)
N2-Tm1-N3	32.8(2)	N8-Tm1-N4^{I}	108.3(2)
N2-Tm1-N4^{I}	82.4(2)	N8-Tm1-N5	80.8(2)
N2-Tm1-N5	80.8(2)	N8-Tm1-N10	84.2(2)
N2-Tm1-N6	85.4(2)	N9-Tm1-N1^{II}	77.6(2)
N2-Tm1-N8	161.4(2)	N9-Tm1-N2	155.4(2)
N2-Tm1-N10	91.9(2)	N9-Tm1-N3	147.8(2)
N3-Tm1-N1^{II}	80.5(2)	N9-Tm1-N4^{I}	75.9(2)
N3-Tm1-N4^{I}	79.9(2)	N9-Tm1-N5	98.9(2)
N3-Tm1-N10	82.4(2)	N9-Tm1-N6	81.4(2)
N4^{I}-Tm1-N1^{II}	87.6(2)	N9-Tm1-N8	32.7(2)
N4^{I}-Tm1-N10	155.3(2)	N9-Tm1-N10	112.6(2)
N5-Tm1-N1^{II}	153.6(2)	N10-Tm1-N1^{II}	72.5(2)
N5-Tm1-N3	111.0(2)		

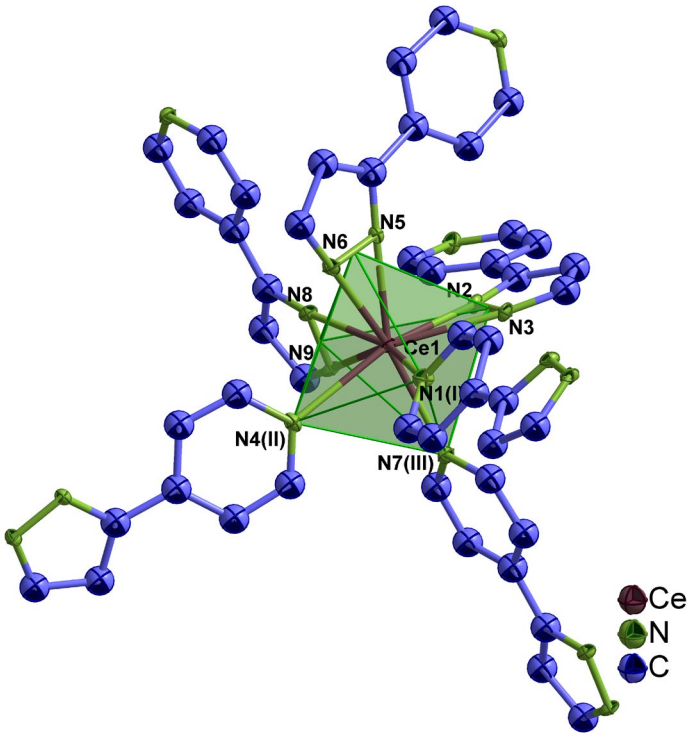

Figure S1. Extended coordination sphere of Ce^{3+} in $^{3}_{\infty}$[Ce(4-PyPz)$_3$] (**4-Ce**) representing the series of isotypic framework compounds (**4**, Ln = La, Ce, Pr, Nd, Ho, Er, Tm). The coordination polyhedra around Ce^{3+} is indicated in green and the thermal ellipsoids describe a 50 % probability level of the atoms. Symmetry operations: I x+1/2,−y+1/2,z+1/2 II −x+3/2,y−1/2,−z+3/2 III x+1,y,z

Table S10. Selected interatomic distances (pm) and angles (◦) of $^{3}_{\infty}$[Ln(4-PyPz)$_3$] (**4**, Ln = La, Ce, Pr, Nd, Ho, Er). Symmetry operations: I x+1/2,−y+1/2,z+1/2 II −x+3/2,y−1/2,−z+3/2 III x+1,y,z

Atoms	**$^{3}_{\infty}$[La(4-PzPy)$_3$]**	**$^{3}_{\infty}$[Ce(4-PzPy)$_3$]**	**$^{3}_{\infty}$[Pr(4-PzPy)$_3$]**	**$^{3}_{\infty}$[Nd(4-PzPy)$_3$]**	**$^{3}_{\infty}$[Ho(4-PzPy)$_3$]**	**$^{3}_{\infty}$[Er(4-PzPy)$_3$]**
Ln1-N2	251.0(3)	248.2(3)	246.3(2)	244.8(2)	236.0(4)	235.2(3)
Ln1-N5	251.3(3)	247.5(3)	246.1(2)	245.0(2)	236.1(3)	235.3(3)
Ln1-N8	251.2(3)	248.1(3)	246.4(2)	245.5(2)	236.9(4)	235.9(4)
Ln1-N9	256.2(3)	254.0(3)	251.8(2)	250.3(2)	241.4(4)	240.6(3)
Ln1-N6	256.8(3)	254.3(3)	252.3(2)	251.2(2)	242.8(4)	241.4(3)
Ln1-N3	259.3(3)	256.7(3)	254.2(2)	252.9(2)	243.8(4)	242.9(3)
Ln1-N1^{I}	267.7(4)	264.9(3)	263.3(2)	262.1(2)	253.3(3)	251.8(3)
Ln1-N4^{II}	269.5(3)	266.8(2)	264.9(2)	264.1(2)	254.5(3)	253.0(3)
Ln1-N7^{III}	269.9(3)	267.1(3)	265.4(2)	264.2(2)	254.2(3)	252.8(3)
N2-Ln1-N5	86.5(1)	86.4(1)	86.3(1)	86.2(1)	86.0(2)	85.6(2)
N2-Ln1-N8	90.5(1)	90.1(1)	90.2(1)	90.3(1)	89.9(2)	89.9(2)
N5-Ln1-N8	84.5(1)	84.4(1)	84.4(1)	84.4(1)	84.5(2)	84.6(2)
N2-Ln1-N9	85.2(1)	85.2(1)	85.1(1)	85.2(1)	84.7(2)	84.8(2)
N5-Ln1-N9	114.7(1)	115(1)	115.3(1)	115.4(1)	116.6(2)	116.6(2)
N8-Ln1-N9	31.1(1)	31.4(1)	31.8(1)	31.9(1)	33.1(2)	33.0(1)
N2-Ln1-N6	117.6(1)	117.8(1)	118.0(1)	118.1(1)	118.8(2)	118.7(2)
N5-Ln1-N6	31.1(1)	31.4(1)	31.7(1)	31.9(1)	32.8(2)	33.1(1)
N8-Ln1-N6	85.7(1)	85.5(1)	85.4(1)	85.2(1)	84.7(2)	84.7(2)
N9-Ln1-N6	115.2(1)	115.2(1)	115.5(1)	115.4(1)	115.9(2)	115.7(2)
N2-Ln1-N3	31.1(1)	31.2(1)	31.4(1)	31.7(1)	32.8(1)	32.9(1)
N5-Ln1-N3	82.7(1)	82.7(1)	82.8(1)	82.7(1)	82.6(2)	82.4(1)

N8-Ln1-N3	120.5(1)	120.4(1)	120.7(1)	121.0(1)	121.8(2)	121.9(2)
N9-Ln1-N3	114.9(1)	115(1)	115.0(1)	115.1(1)	115.5(2)	115.6(2)
N6-Ln1-N3	108.9(1)	109.2(1)	109.4(1)	109.6(1)	110.4(2)	110.4(1)
N2-Ln1-N1^{I}	115.1(1)	115(1)	115.2(1)	115.2(1)	115.5(2)	115.4(2)
N5-Ln1-N1^{I}	88.8(1)	88.3(1)	88.3(1)	88.2(1)	87.2(2)	87.0(1)
N8-Ln1-N1^{I}	153.1(1)	153.4(1)	153.0(1)	152.9(1)	152.6(2)	152.6(2)
N9-Ln1-N1^{I}	150.6(1)	150.9(1)	150.6(1)	150.6(1)	150.6(2)	151.0(1)
N6-Ln1-N1^{I}	75.5(1)	75.2(1)	75.0(1)	75.0(1)	74.4(2)	74.2(2)
N3-Ln1-N1^{I}	84.1(1)	83.8(1)	83.9(1)	83.6(1)	82.7(2)	82.5(1)
N2-Ln1-N4^{II}	156.1(1)	156.2(1)	155.6(1)	155.5(1)	154.9(2)	155.1(1)
N5-Ln1-N4^{II}	114.4(1)	114.3(1)	114.8(1)	115.2(1)	115.5(1)	115.8(1)
N8-Ln1-N4^{II}	80.7(1)	80.7(1)	80.5(1)	80.6(1)	80.2(2)	80.2(2)
N9-Ln1-N4^{II}	75.7(1)	75.5(1)	75.1(1)	75.1(1)	74.4(2)	74.4(1)
N6-Ln1-N4^{II}	84.1(1)	83.6(1)	83.9(1)	84.0(1)	83.4(2)	83.3(1)
N3-Ln1-N4^{II}	155.1(1)	155.2(1)	154.9(1)	154.4(1)	154.0(1)	153.9(1)
N1^{I}-Ln1-N4^{II}	78.6(1)	79.0(1)	79.1(1)	79.0(1)	80.0(2)	80.2(1)
N2-Ln1-N7^{III}	81.2(1)	81.1(1)	80.9(1)	80.9(1)	80.6(2)	80.8(1)
N5-Ln1-N7^{III}	158(1)	158(1)	157.5(1)	157.0(1)	155.6(1)	155.4(2)
N8-Ln1-N7^{III}	113.6(1)	113.5(1)	113.9(1)	114.5(1)	115.7(2)	115.6(2)
N9-Ln1-N7^{III}	82.5(1)	82.1(1)	82.1(1)	82.6(1)	82.5(2)	82.6(2)
N6-Ln1-N7^{III}	153.9(1)	154.1(1)	153.8(1)	153.5(1)	153.0(2)	153.0(2)
N3-Ln1-N7^{III}	77.3(1)	77.2(1)	76.7(1)	76.3(1)	75.0(1)	75.0(1)
N1^{I}-Ln1-N7^{III}	80.2(1)	80.8(1)	80.6(1)	80.2(1)	80.3(2)	80.6(2)
N4^{II}-Ln1-N7^{III}	82.2(1)	82.5(1)	82.3(1)	82.3(1)	83.0(1)	83.0(1)

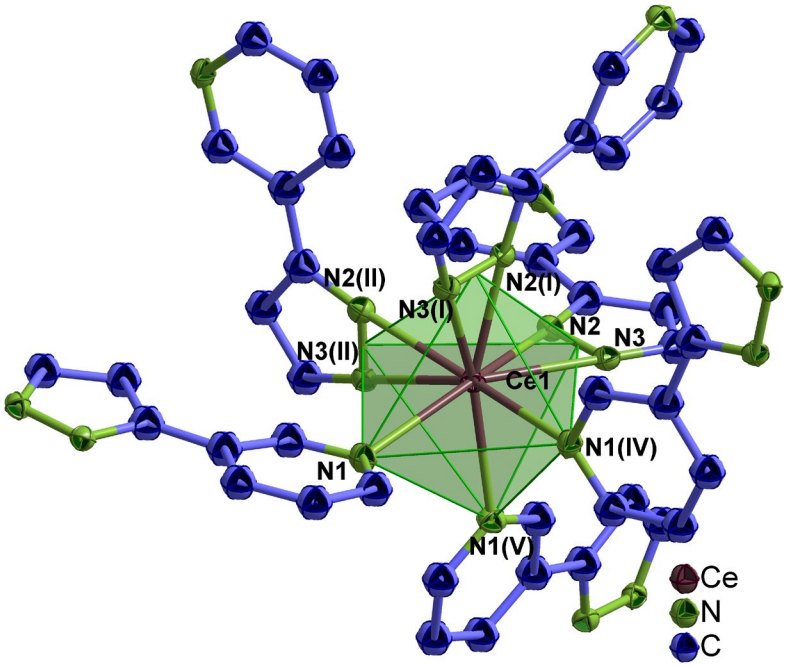

Figure S2. Extended coordination sphere of Ce^{3+} in $^{3}_{\infty}$[Ce(3-PyPz)$_3$] (**3-Ce**) representing the series of isotypic framework compounds (**3**, Ln = Ce, Pr, Nd, Ho, Er, Tm). The coordination polyhedra around Ce^{3+} is indicated in green and the thermal ellipsoids describe a 50 % probability level of the atoms. Symmetry operations: I −z+1,x+1/2,−y+3/2 II y−1/2,−z+3/2, −x+1 III x−1/2,y,−z+3/2 IV y−1/2,z,−x+3/2 V z−1/2,x,−y+3/2.

Table S11. Selected interatomic distances (pm) and angles (◦) of $^{3}_{\infty}$[Ln(3-PyPz)$_3$], (**3**, Ln = Ce, Pr, Nd, Ho, Er,Tm). Symmetry operations: I −z+1,x+1/2,−y+3/2 II y−1/2,−z+3/2,−x+1 III x−1/2,y,−z+3/2 IV y−1/2,z,−x+3/2 V z−1/2,x,−y+3/2.

Atoms	**$^{3}_{\infty}$[Ce(3-PyPz)$_3$]**	**$^{3}_{\infty}$[Pr(3-PyPz)$_3$]**	**$^{3}_{\infty}$[Nd(3-PyPz)$_3$]**	**$^{3}_{\infty}$[Ho(3-PyPz)$_3$]**	**$^{3}_{\infty}$[Er(3-PyPz)$_3$]**	**$^{3}_{\infty}$[Tm(3-PyPz)$_3$]**
Ln1-N2	246.6(3)	245.0(2)	243.5(2)	235.2(2)	234.2(2)	233.6(5)
Ln1-N3	252.7(3)	250.3(2)	249.0(2)	239.8(2)	238.6(2)	238.3(5)
Ln1-N1^{III}	268.7(3)	267.1(2)	265.4(2)	256.0(2)	255.0(2)	254.2(5)
N2-Ln1-N2^{I}	85.6(1)	85.5(1)	85.6(1)	85.8(1)	85.8(1)	86.0(2)
N2-Ln1-N3	31.9(1)	32.1(1)	32.3(1)	33.3(1)	33.5(1)	33.4(2)
N2^{I}-Ln1-N3	82.6(1)	82.6(1)	82.8(1)	83.0(1)	82.9(1)	83.0(2)
N2^{II}-Ln1-N3	116.9(1)	117.0(1)	117.3(1)	118.6(1)	118.7(1)	118.8(2)
N3-Ln1-N3^{II}	112.3(1)	112.5(1)	112.7(1)	113.5(1)	113.7(1)	113.6(1)
N2-Ln1-N1^{III}	161.3(1)	161.2(1)	161.4(1)	161.6(1)	161.6(1)	161.9(2)
N2^{I}-Ln1-N1^{III}	109.7(1)	109.9(1)	109.7(1)	109.4(1)	109.4(1)	109.0(2)
N2^{II}-Ln1-N1^{III}	84.9(1)	85.1(1)	85.1(1)	85.0(1)	85.0(1)	85.0(2)
N3-Ln1-N1^{III}	156.4(1)	156.0(1)	155.7(1)	154.7(1)	154.6(1)	154.7(2)
N3^{II}-Ln1-N1^{III}	80.8(1)	80.8(1)	80.8(1)	80.6(1)	80.6(1)	80.8(2)
N3^{I}-Ln1-N1^{III}	77.7(1)	77.8(1)	77.4(1)	76.0(1)	75.9(1)	75.6(2)
N1^{III}-Ln1-N1^{IV}	83.2(1)	82.9(1)	82.8(1)	83.0(1)	83.0(1)	83.1(2)

Powder Diffraction

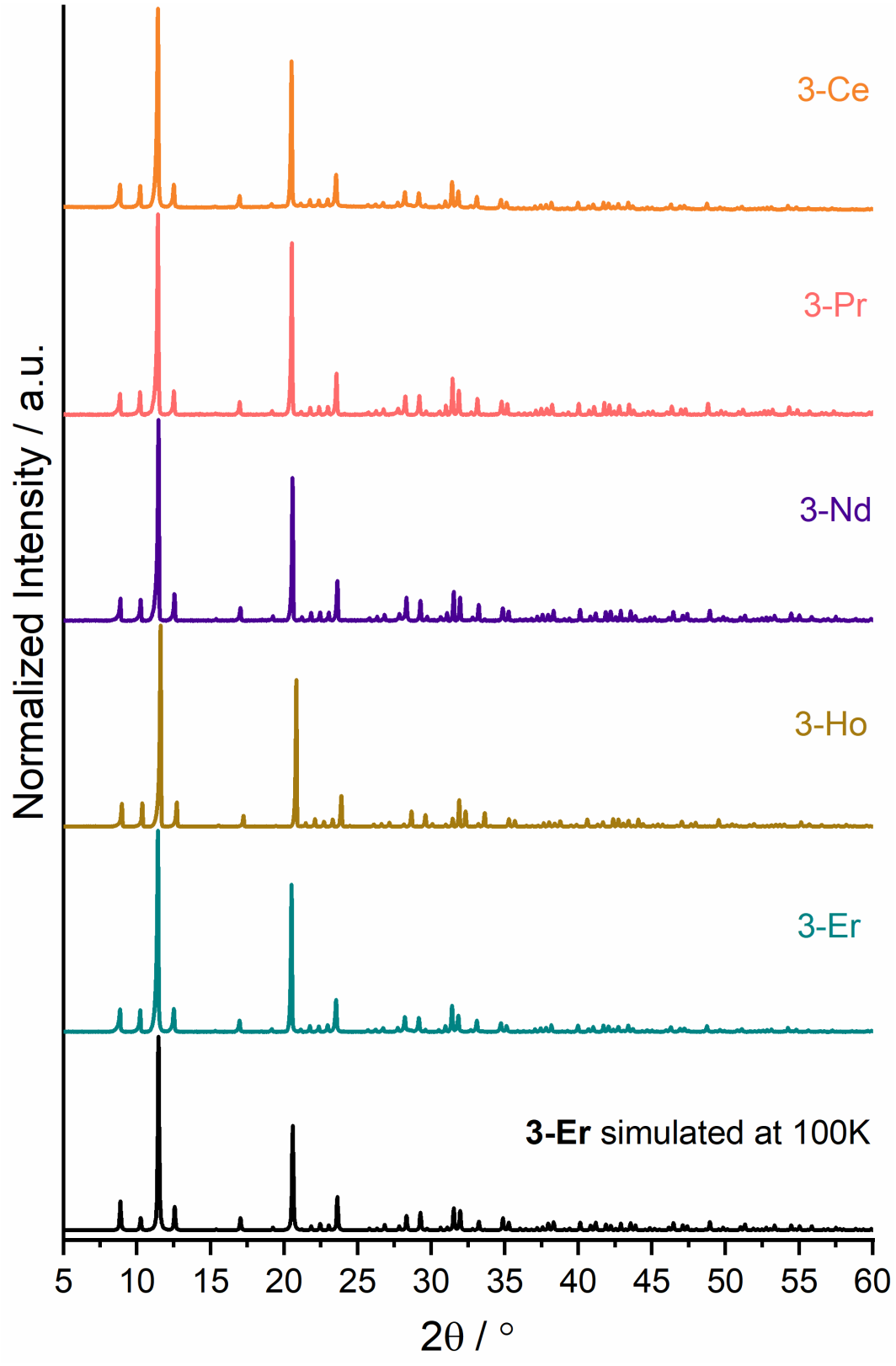

Figure S3. Comparison of the experimental X-ray powder diffraction pattern of $^{3}_{\infty}$[Ln(3-PyPz)$_3$] (**3**, Ln = Pr, Nd, Ho, Er, Tm) at RT with the simulated pattern from the single-crystal X-ray data of $^{3}_{\infty}$[Er(3-PyPz)$_3$] (**3-Er**) at 100 K.

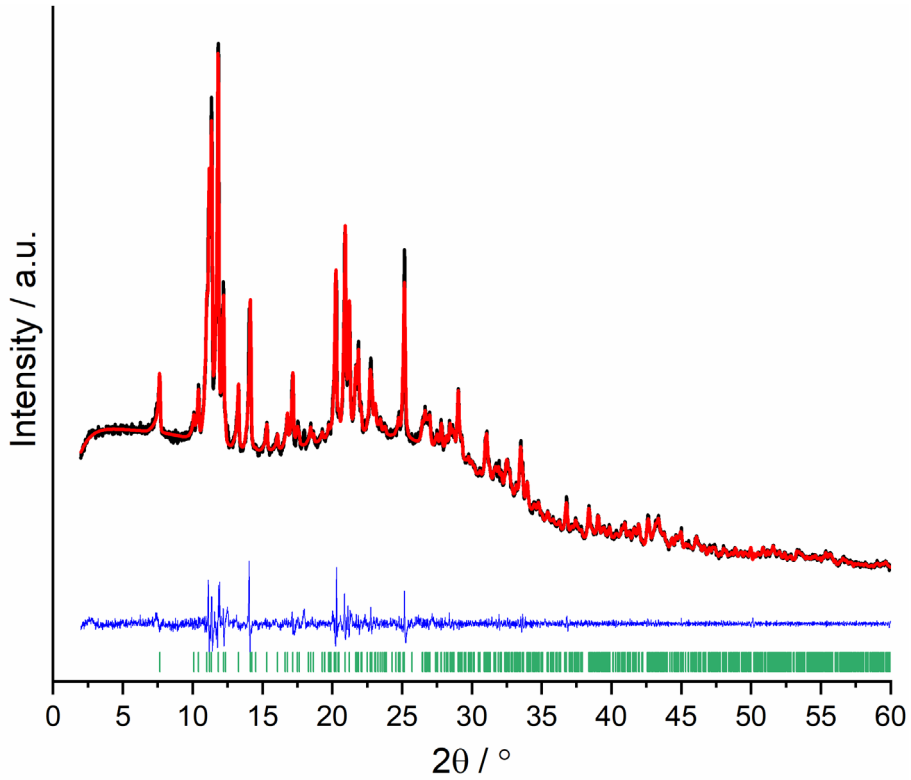

Figure S4. Pawley refinement results for PXRD of $^{3}_{\infty}$[La(4-PyPz)$_3$] (**4-La**), showing the experimental data (black) together with the Pawley fit (red), the corresponding difference plot (blue) as well as hkl position markers (green).

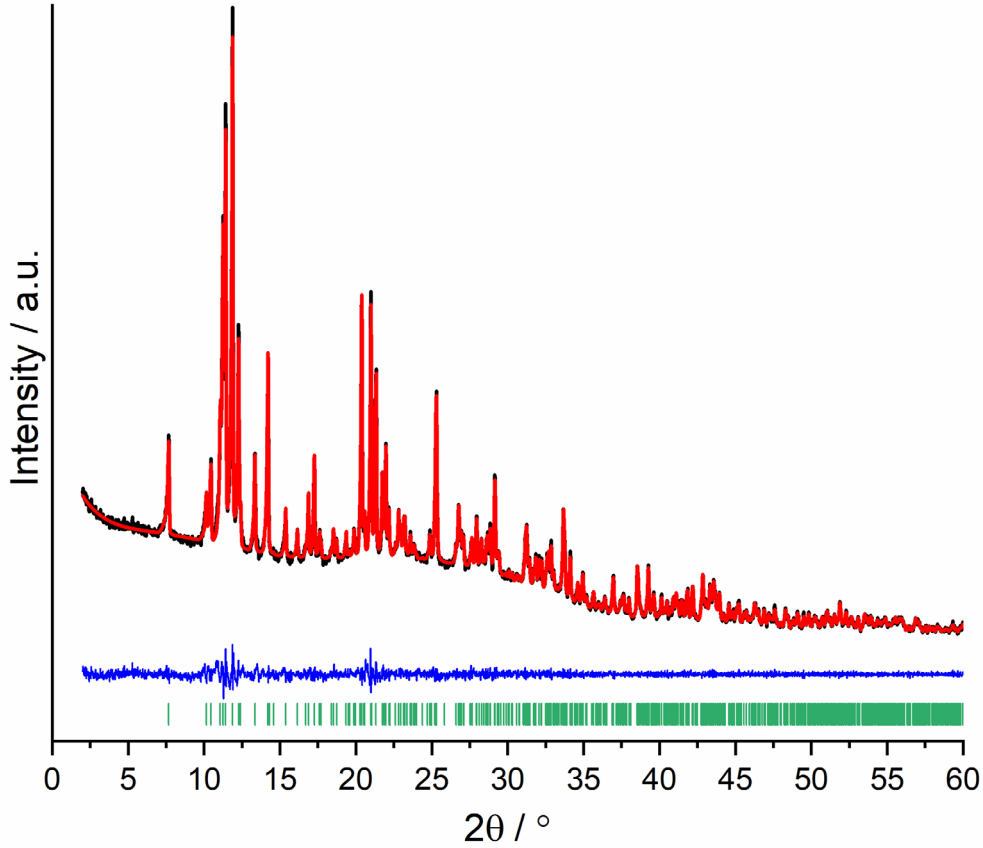

Figure S5. Pawley refinement results for PXRD of $^{3}_{\infty}$[Pr(4-PyPz)$_3$] (**4-Pr**), showing the experimental data (black) together with the Pawley fit (red), the corresponding difference plot (blue) as well as hkl position markers (green).

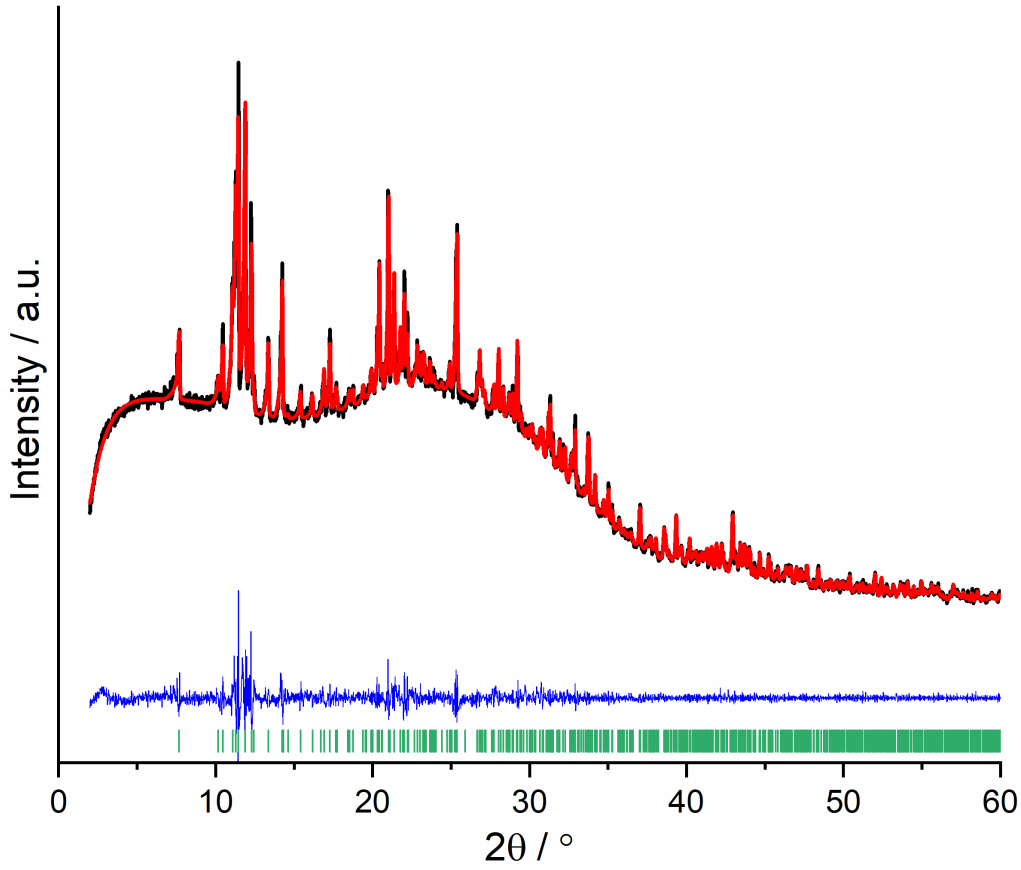

Figure S6. Pawley refinement results for PXRD of $^{3}_{\infty}$[Nd(4-PyPz)$_3$] (**4-Nd**), showing the experimental data (black) together with the Pawley fit (red), the corresponding difference plot (blue) as well as hkl position markers (green).

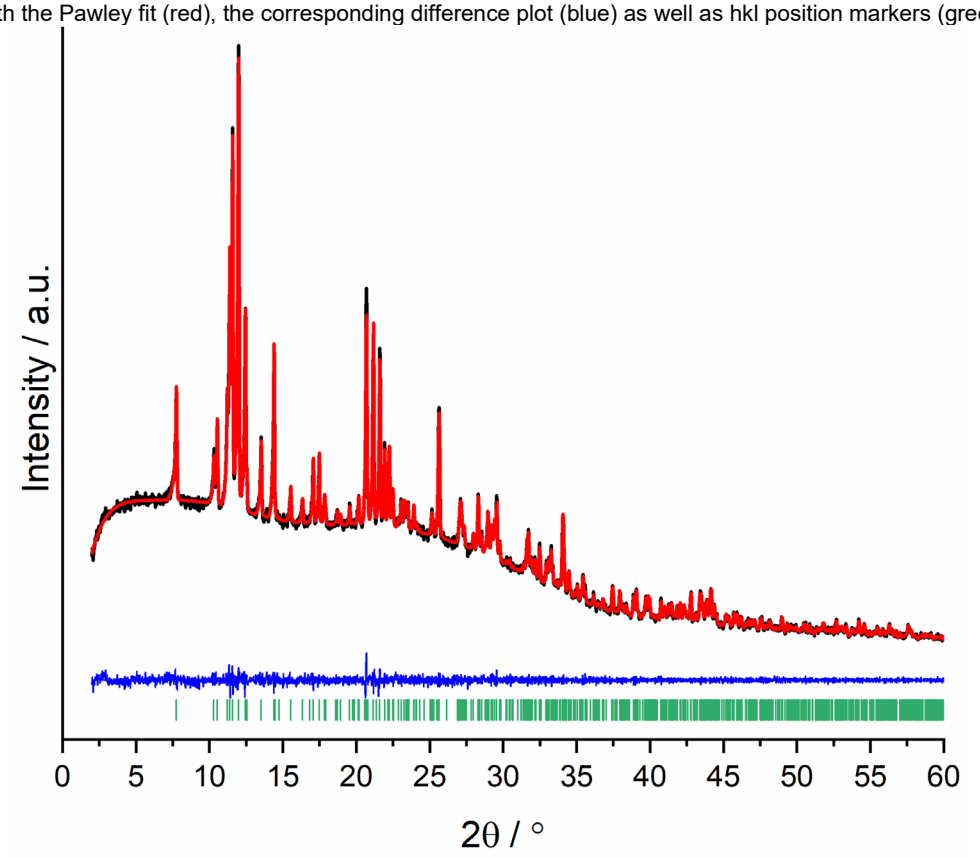

Figure S7. Pawley refinement results for PXRD of $^{3}_{\infty}$[Ho(4-PyPz)$_3$] (**4-Ho**), showing the experimental data (black) together with the Pawley fit (red), the corresponding difference plot (blue) as well as hkl position markers (green).

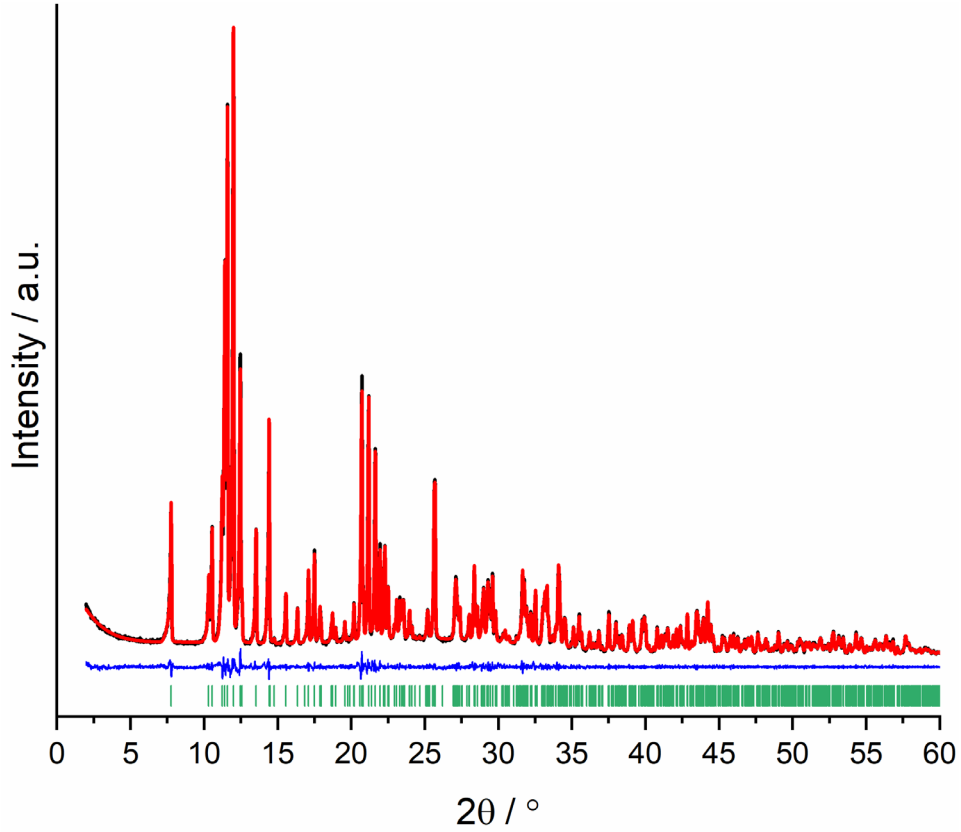

Figure S8. Pawley refinement results for PXRD of $^{3}_{\infty}$[Er(4-PyPz)$_3$] (**4-Er**), showing the experimental data (black) together with the Pawley fit (red), the corresponding difference plot (blue) as well as hkl position markers (green).

Table S12. Pawley refinement results for $^{2}_{\infty}$[Eu(4-PyPz)$_2$(Py)$_2$] (**4-Eu^{2+}**), $^{2}_{\infty}$[Ce(4-PyPz)$_3$(Py)] (**4-$^{2}_{\infty}$Ce**), and $^{3}_{\infty}$[Ln(4-PyPz)$_3$] (**4**, Ln = La, Pr, Nd, Ho, Er, Tm).

Compound	**$^{2}_{\infty}$[Eu(4-PyPz)$_2$(Py)$_2$]**	**$^{2}_{\infty}$[Ce(4-PyPz)$_3$(Py)]**	**$^{3}_{\infty}$[La(4-PyPz)$_3$]**	**$^{3}_{\infty}$[Pr(4-PyPz)$_3$]**
R_{wp}	2.7359	4.3334	2.3996	2.4706
GOF	1.3696	1.0395	1.6364	1.0812
Compound	**$^{3}_{\infty}$[Nd(4-PyPz)$_3$]**	**$^{3}_{\infty}$[Ho(4-PyPz)$_3$]**	**$^{3}_{\infty}$[Er(4-PyPz)$_3$]**	**$^{3}_{\infty}$[Tm(4-PyPz)$_3$]**
R_{wp}	2.1610	2.0778	3.7015	2.8265
GOF	1.7183	1.0298	1.2168	1.5827

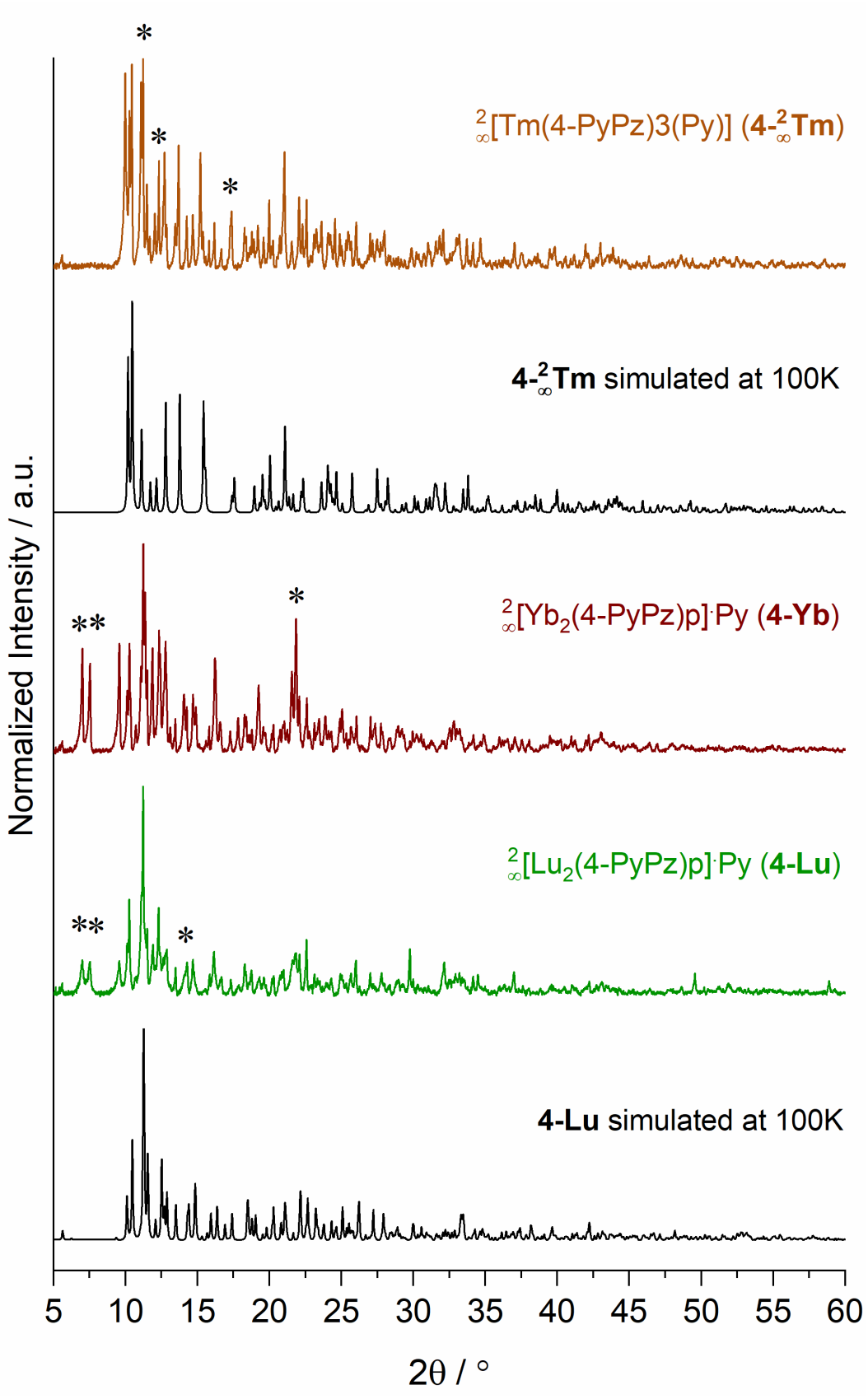

Figure S9. Comparison of the experimental X-ray powder diffraction pattern of $^{2}_{\infty}$[Tm(4-PyPz)$_3$(Py)] (**4-$^{2}_{\infty}$Tm**), $^{2}_{\infty}$[Ln$_2$(4-PyPzH)$_6$]·Py, Ln =Yb (**4-Yb**) and Lu (**4-Lu**) at RT with the respective simulated pattern from single-crystal X-ray data at 100 K.

Photophysical Properties

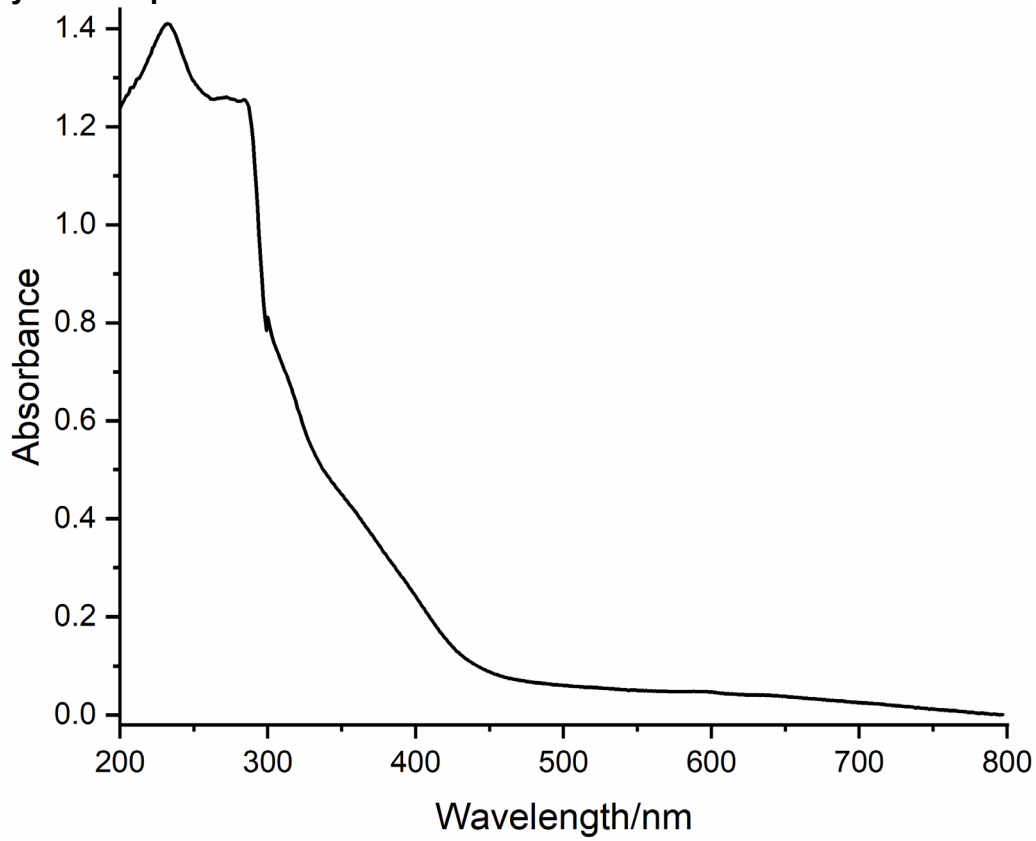

Figure S10. Absorption spectra of **4-PyPzH** in the solid state at room temperature.

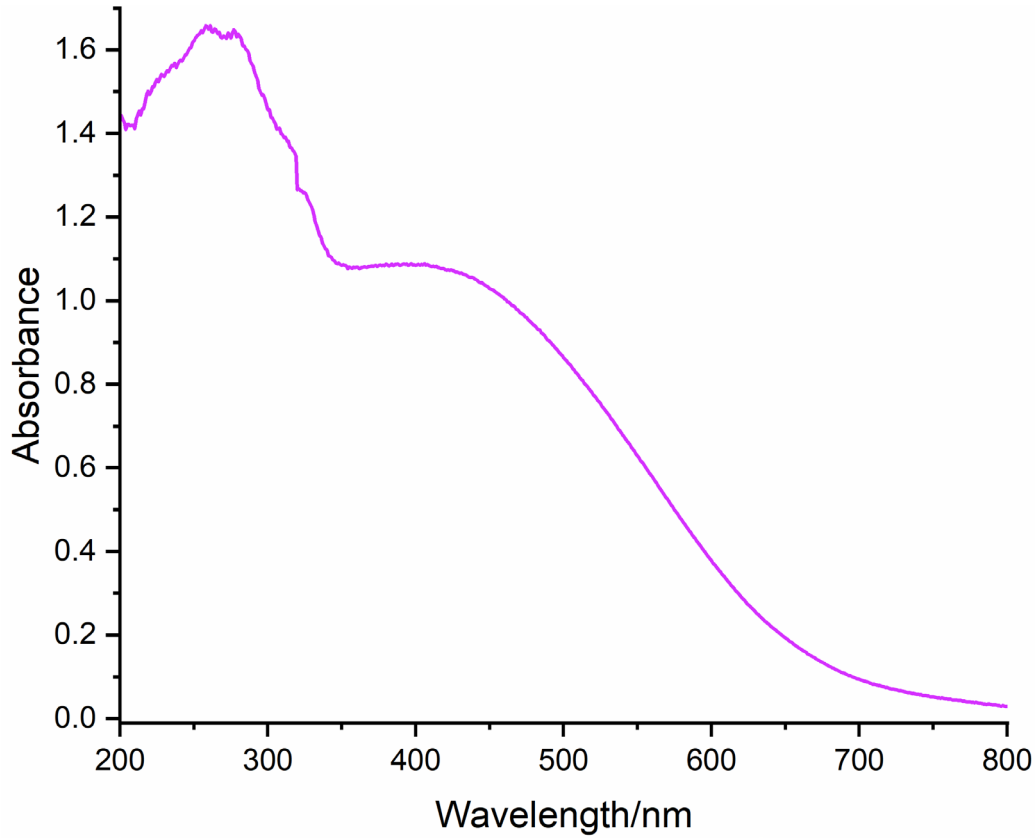

Figure S11. Absorption spectra of $^{2}_{\infty}$[Eu(4-PyPz)$_2$(Py)$_2$] (**4-Eu^{2+}**) in the solid state at room temperature.

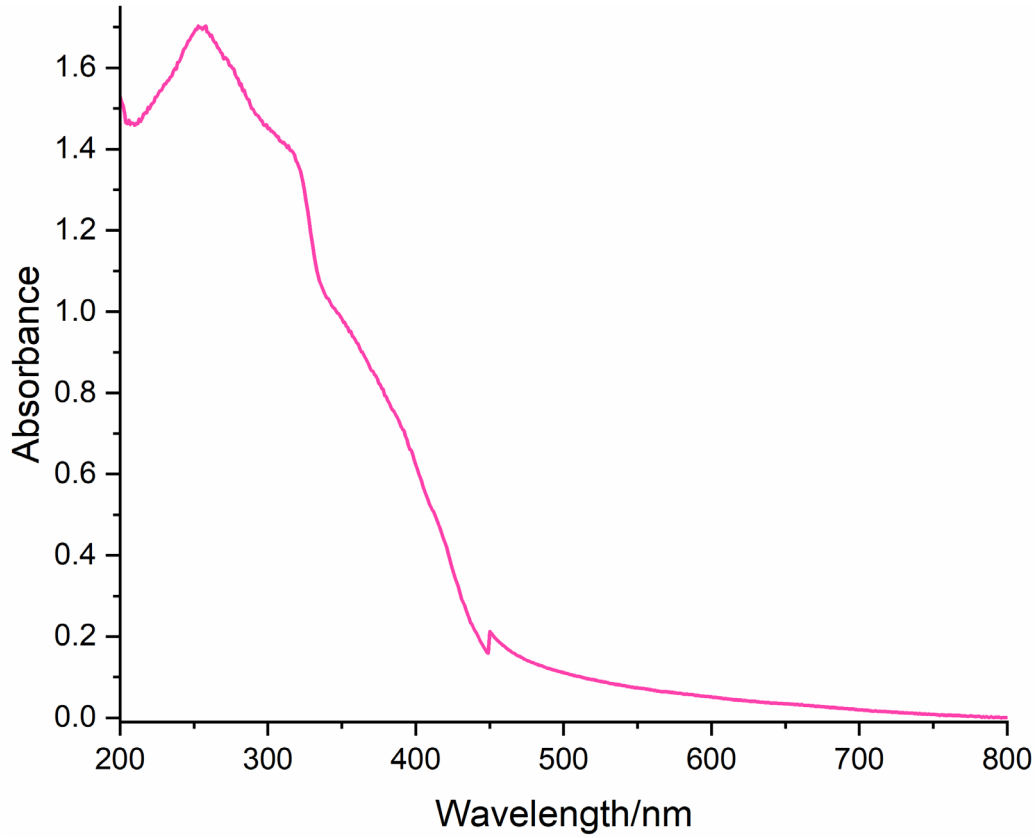

Figure S12. Absorption spectra of $^{2}_{\infty}$[Ce(4-PyPz)$_3$(Py)] (**4-$^{2}_{\infty}$Ce**) in the solid state at room temperature.

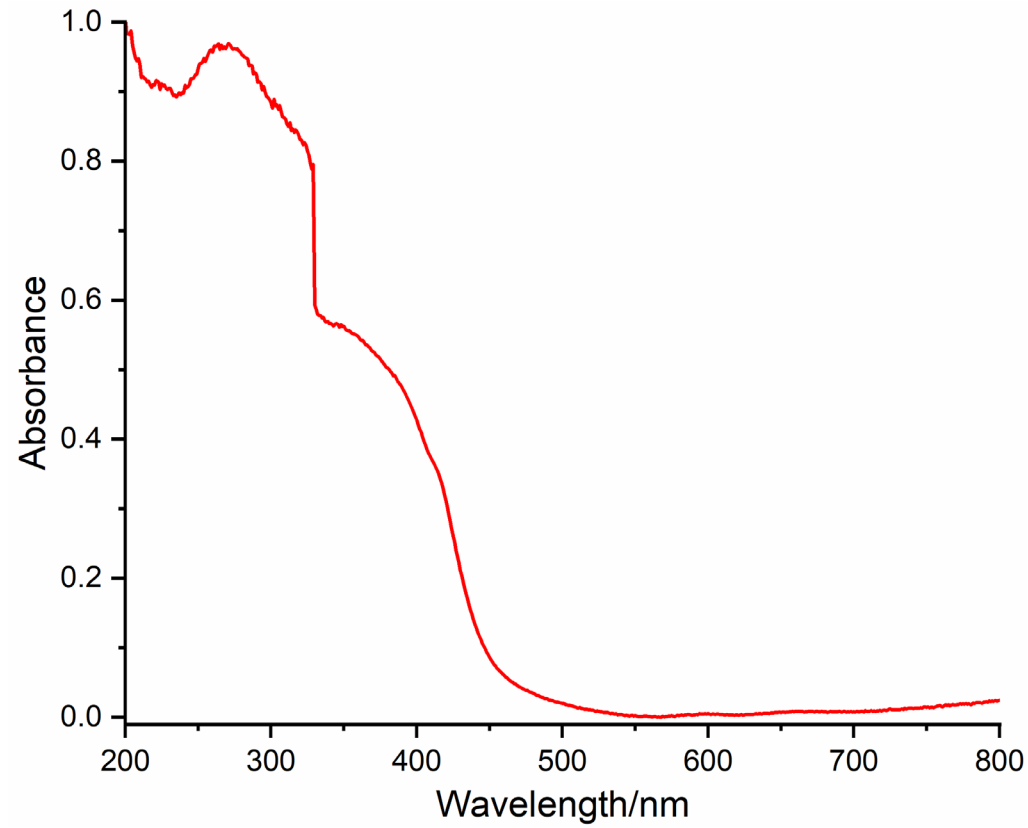

Figure S13. Absorption spectra of $^{3}_{\infty}$[Ce(4-PyPz)$_3$] (**4-Ce**) in the solid state at room temperature.

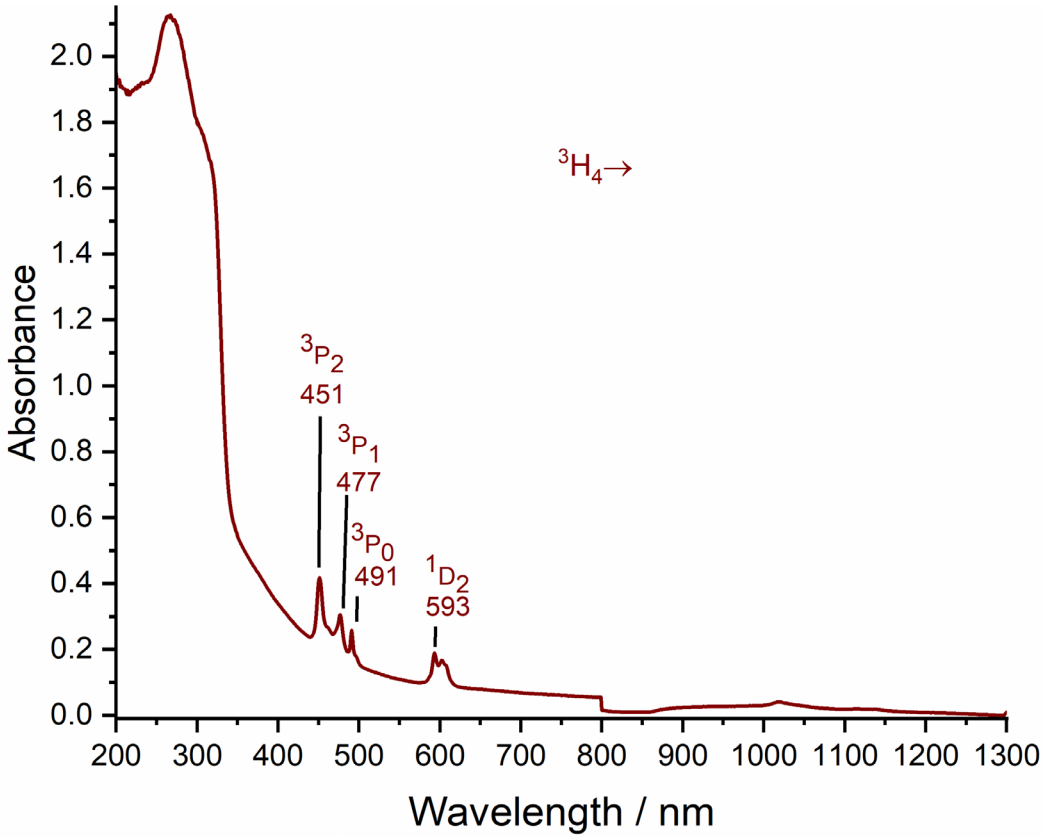

Figure S14. Absorption spectra of $^3_\infty$[Pr(4-PyPz)$_3$] (**4-Pr**) in the solid state at room temperature.

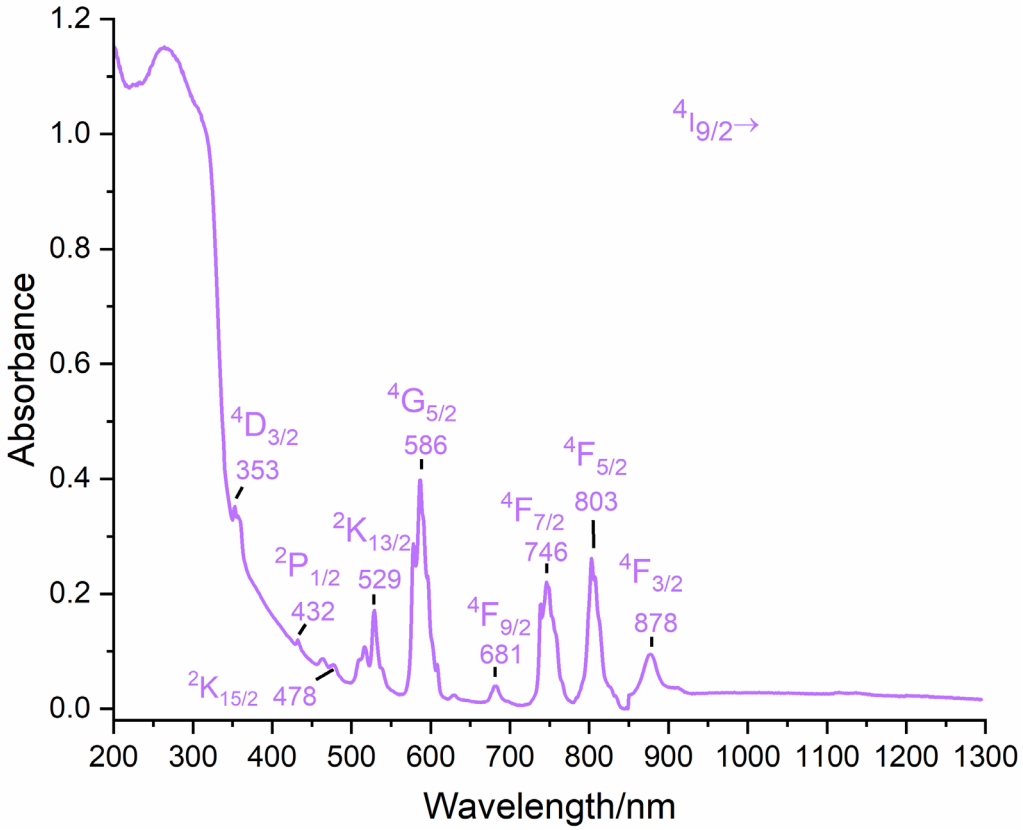

Figure S15. Absorption spectra of $^3_\infty$[Nd(4-PyPz)$_3$] (**4-Nd**) in the solid state at room temperature.

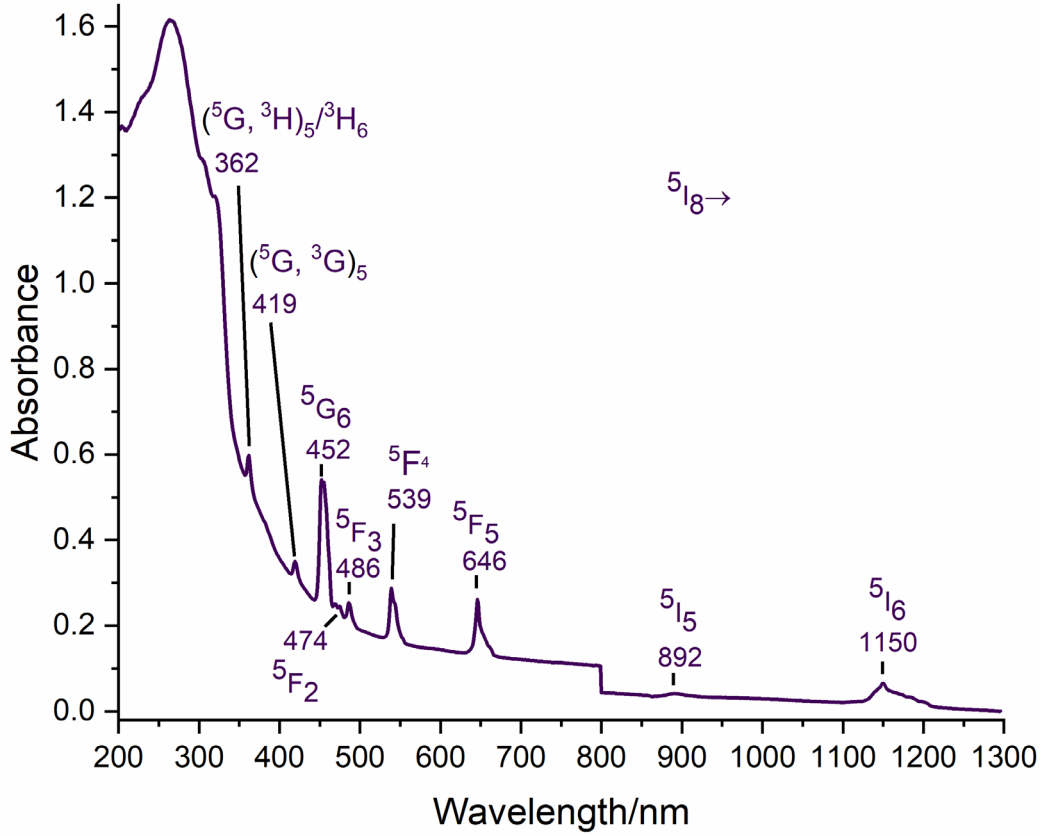

Figure S16. Absorption spectra of $^3_\infty$[Ho(4-PyPz)$_3$] (**4-Ho**) in the solid state at room temperature.

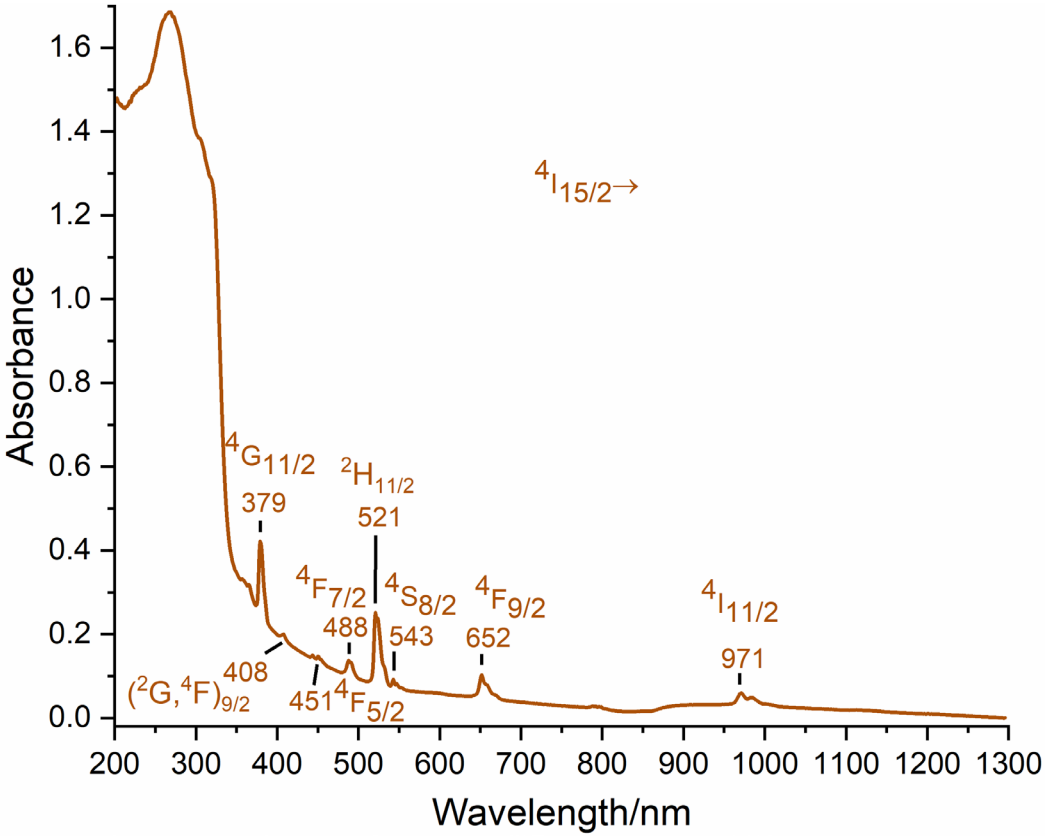

Figure S17. Absorption spectra of $^3_\infty$[Er(4-PyPz)$_3$] (**4-Er**) in the solid state at room temperature.

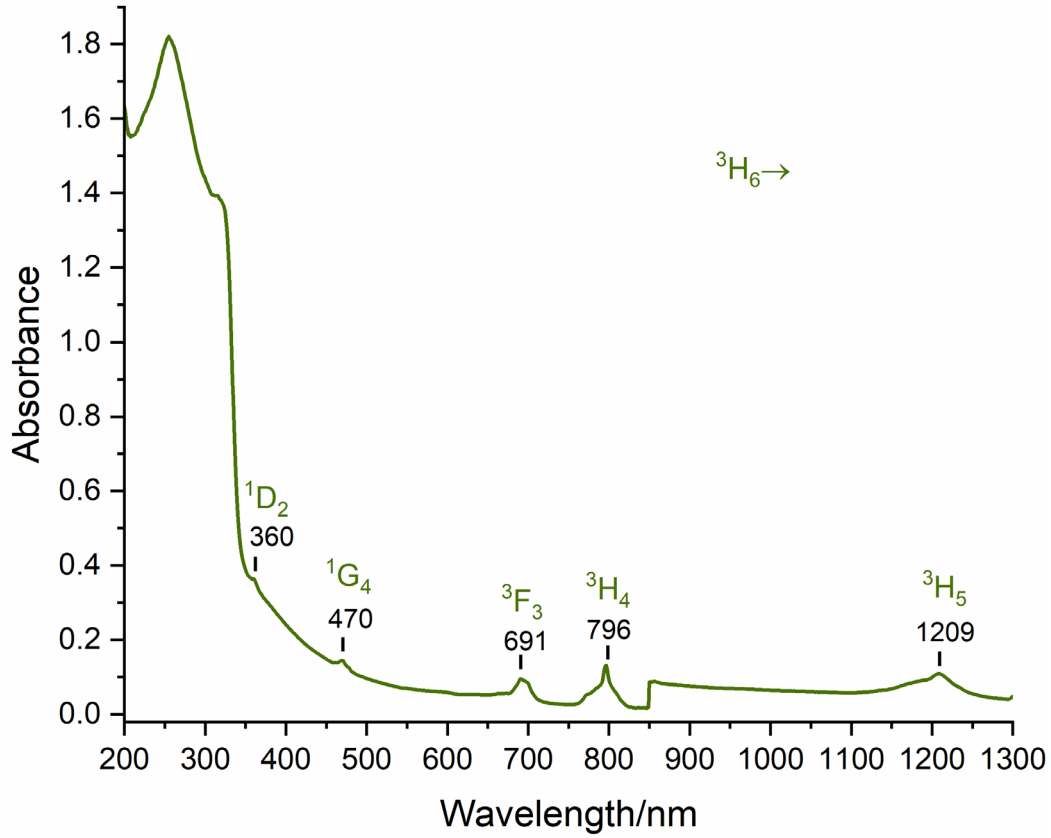

Figure S18. Absorption spectra of $^3_\infty$[Tm(4-PyPz)$_3$] (**4-Tm**) in the solid state at room temperature.

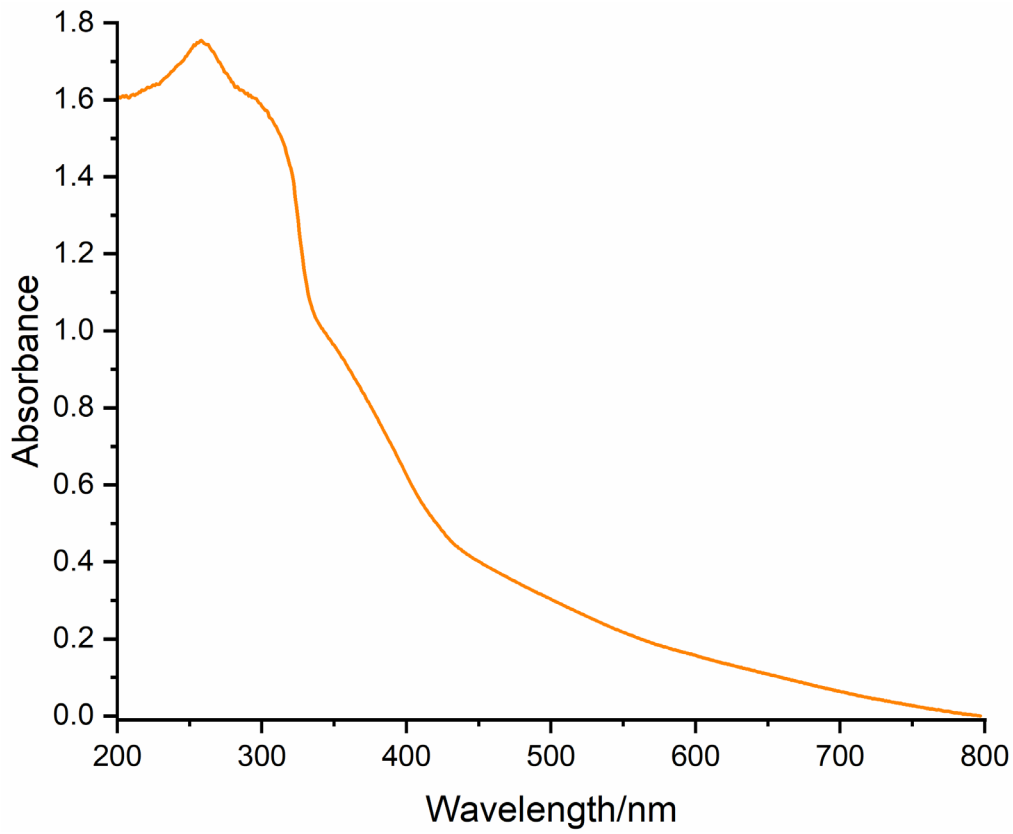

Figure S19. Absorption spectra of $^3_\infty$[Ce(3-PyPz)$_3$] (**3-Ce**) in the solid state at room temperature.

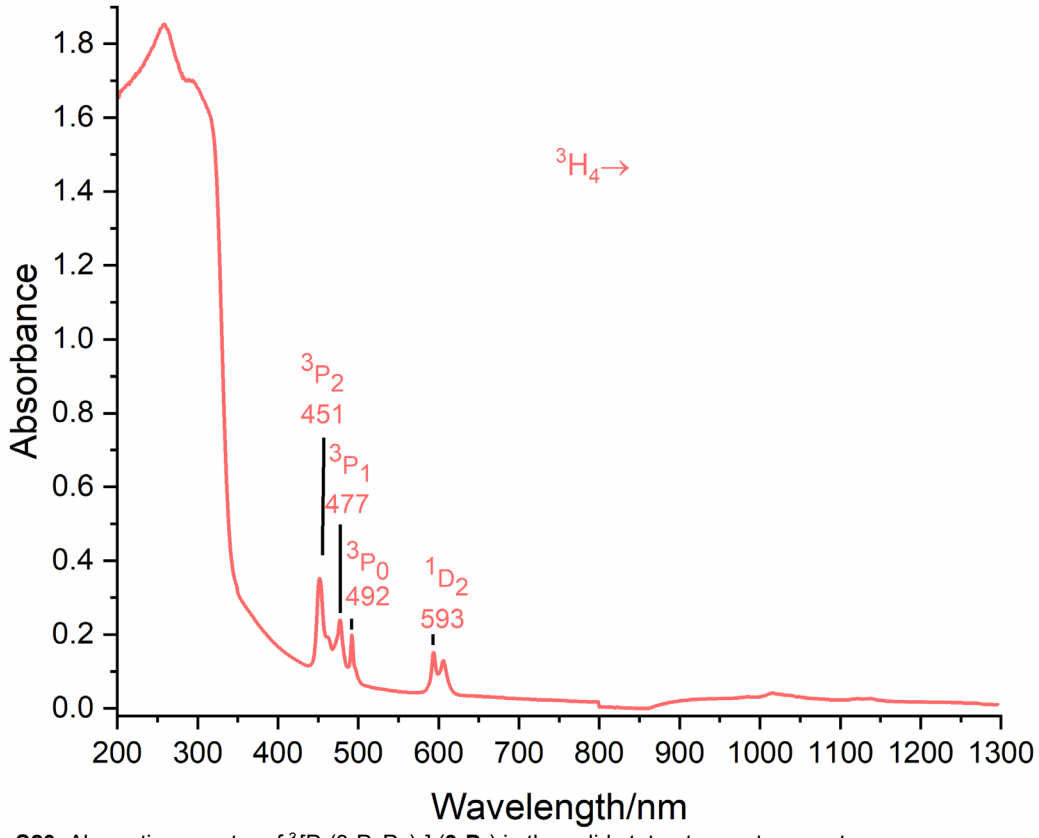

Figure S20. Absorption spectra of $^3_\infty$[Pr(3-PyPz)$_3$] (**3-Pr**) in the solid state at room temperature.

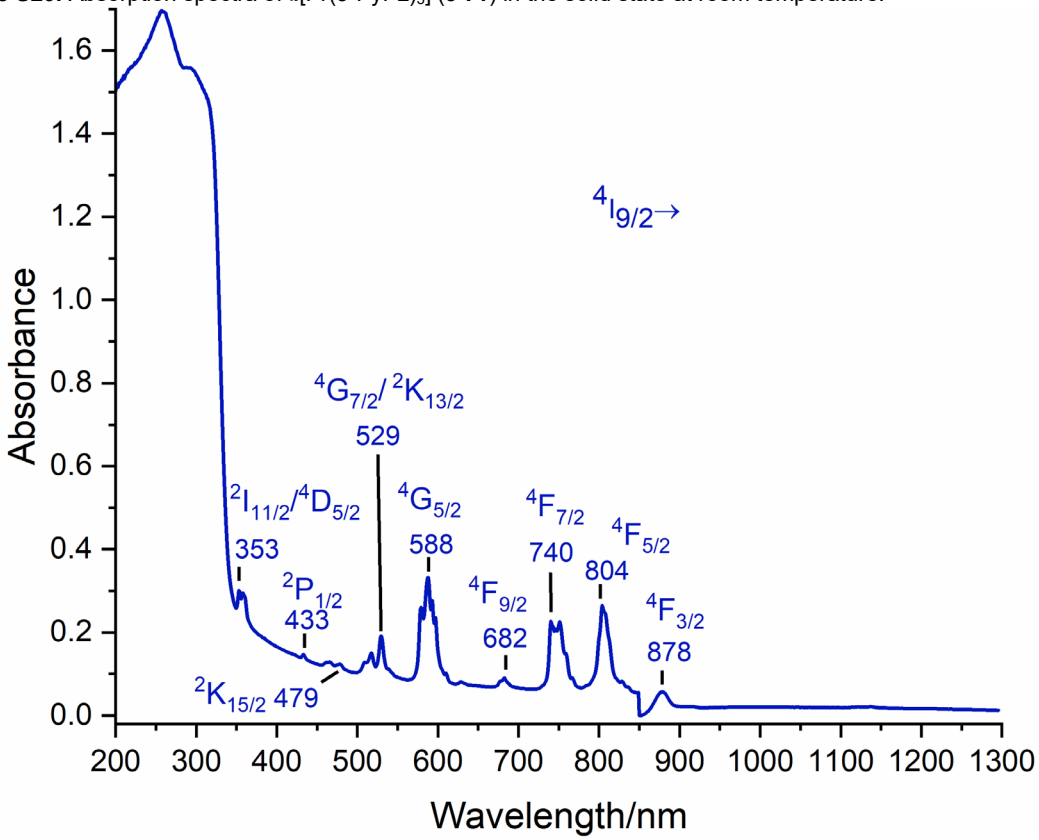

Figure S21. Absorption spectra of $^3_\infty$[Nd(3-PyPz)$_3$] (**3-Nd**) in the solid state at room temperature.

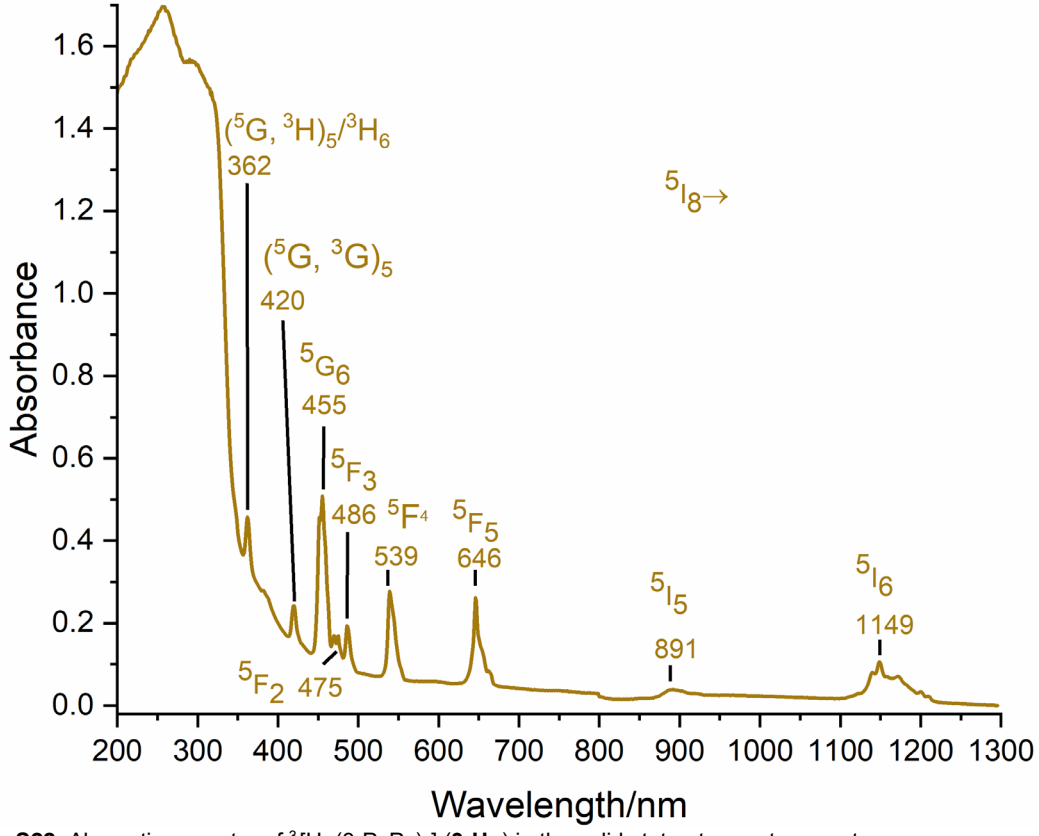

Figure S22. Absorption spectra of $^3_\infty$[Ho(3-PyPz)$_3$] (**3-Ho**) in the solid state at room temperature.

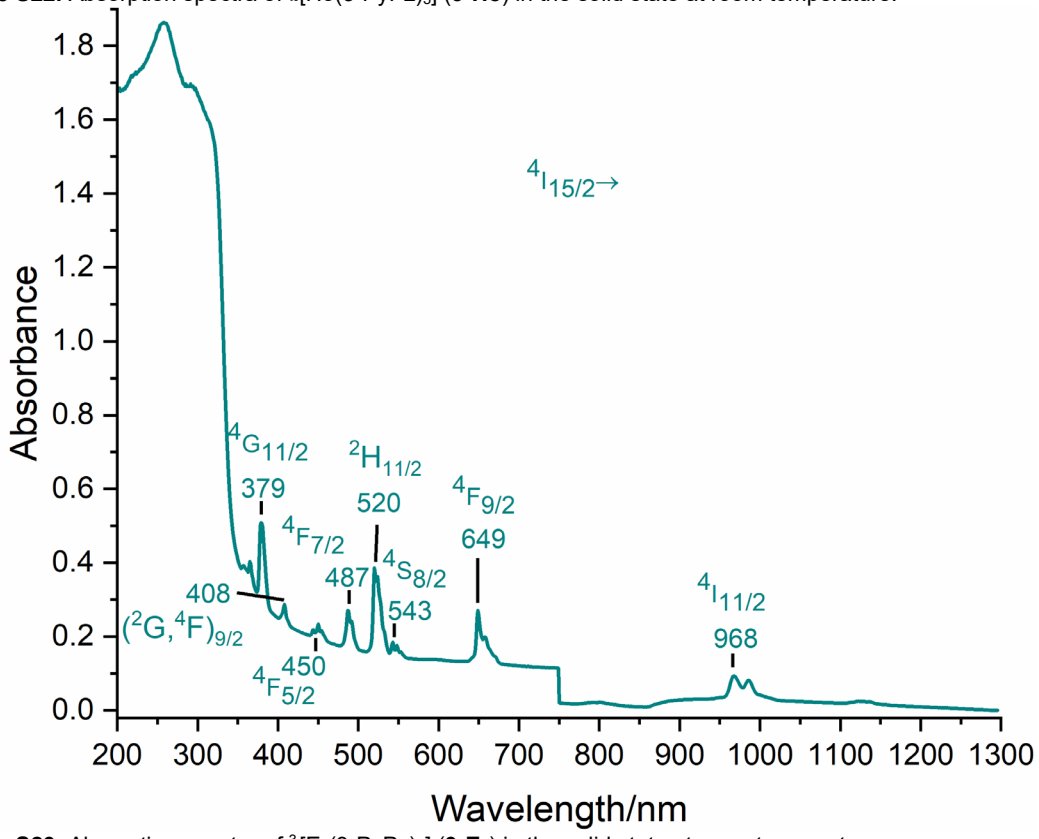

Figure S23. Absorption spectra of $^3_\infty$[Er(3-PyPz)$_3$] (**3-Er**) in the solid state at room temperature.

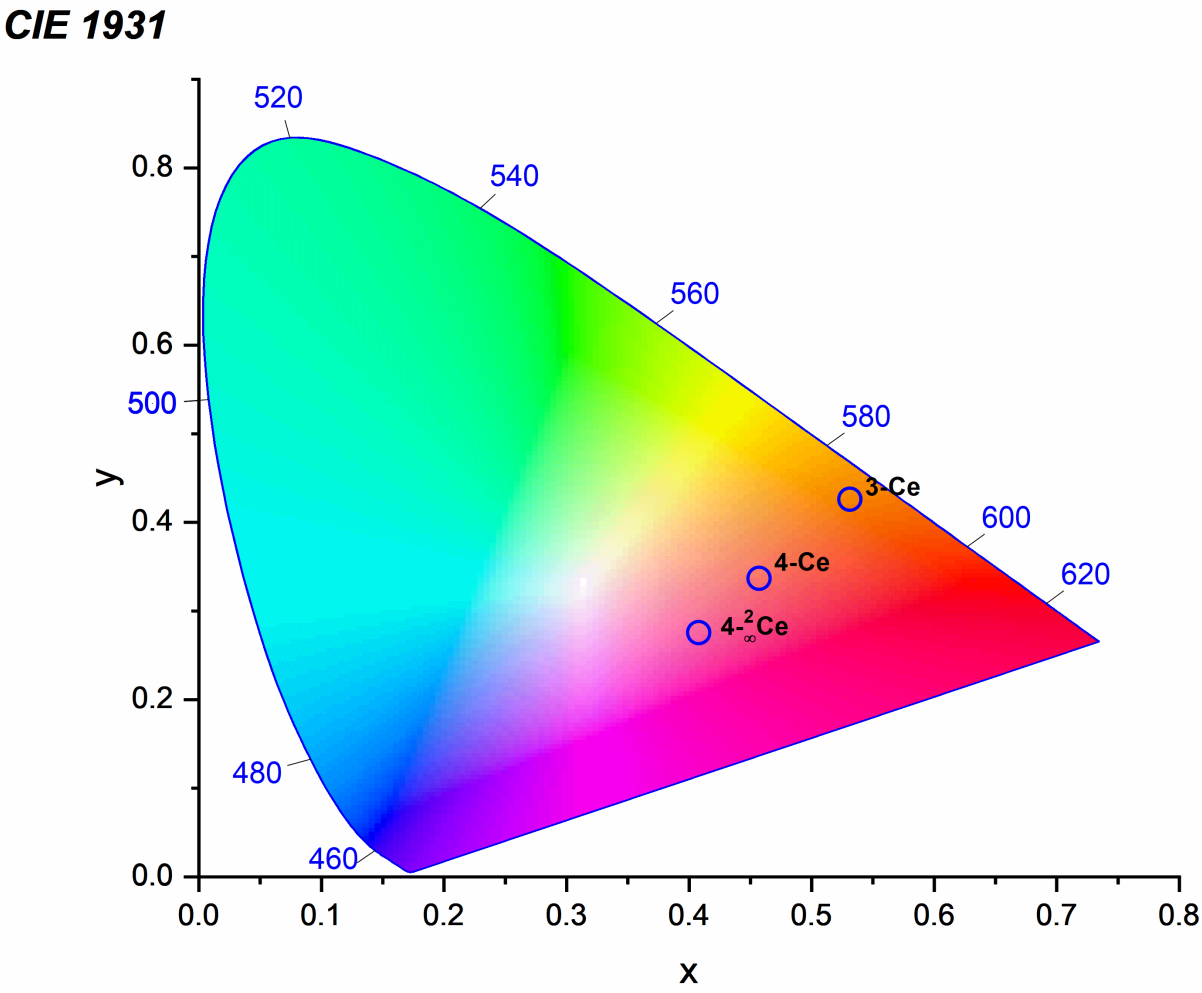

Figure S24. Chromaticity coordinate diagram (CIE 1931) of the emission colors of $^{2}_{\infty}$[Ce(4-PyPz)$_3$(Py)] (**4-$^{2}_{\infty}$Ce**), $^{3}_{\infty}$[Ce(4-PyPz)$_3$] (**4-Ce**) and $^{3}_{\infty}$[Ce(3-PyPz)$_3$] (**3-Ce**).

Table S13. Chromaticity coordinates (x,y) for $^{2}_{\infty}$[Ce(4-PyPz)$_3$(Py)] (**4-$^{2}_{\infty}$Ce**), $^{3}_{\infty}$[Ce(4-PyPz)$_3$] (**4-Ce**), and $^{3}_{\infty}$[Ce(3-PyPz)$_3$] (**3-Ce**).

compound		CIE, x	CIE, y
$^{2}_{\infty}$[Ce(4-PyPz)$_3$(Py)]	**4-$^{2}_{\infty}$Ce**	0.40748	0.27594
$^{3}_{\infty}$[Ce(4-PyPz)$_3$]	**4-Ce**	0.45714	0.33718
$^{3}_{\infty}$[Ce(3-PyPz)$_3$]	**3-Ce**	0.53121	0.42624

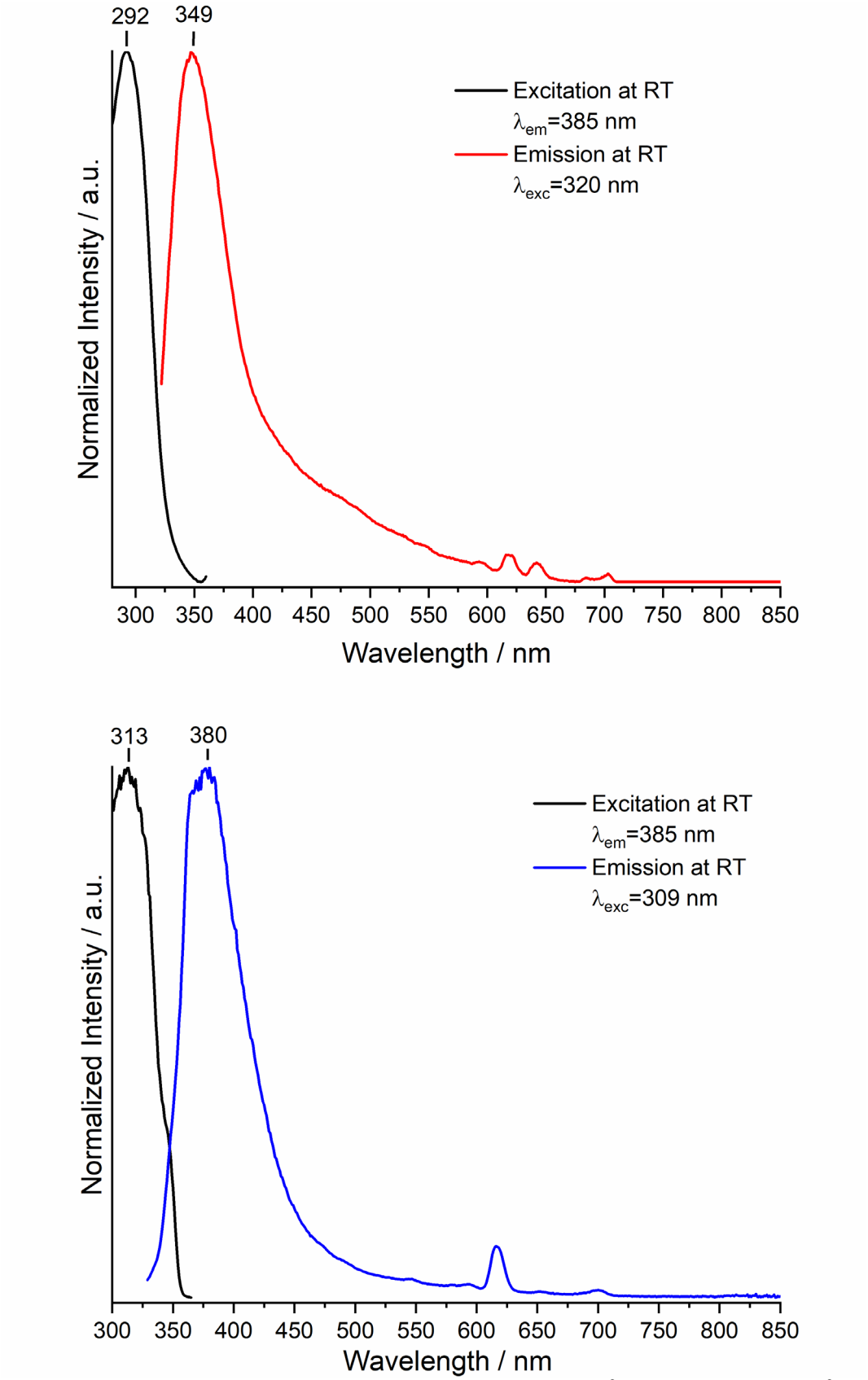

Figure S25. Normalized excitation and normalized emission spectra of $^{2}_{\infty}$[Eu(4-PyPz)$_2$(Py)$_2$] (**4-Eu^{2+}**) at room temperature (top) and 77K (bottom). Wavelengths at which the spectra were recorded are reported in the legends.

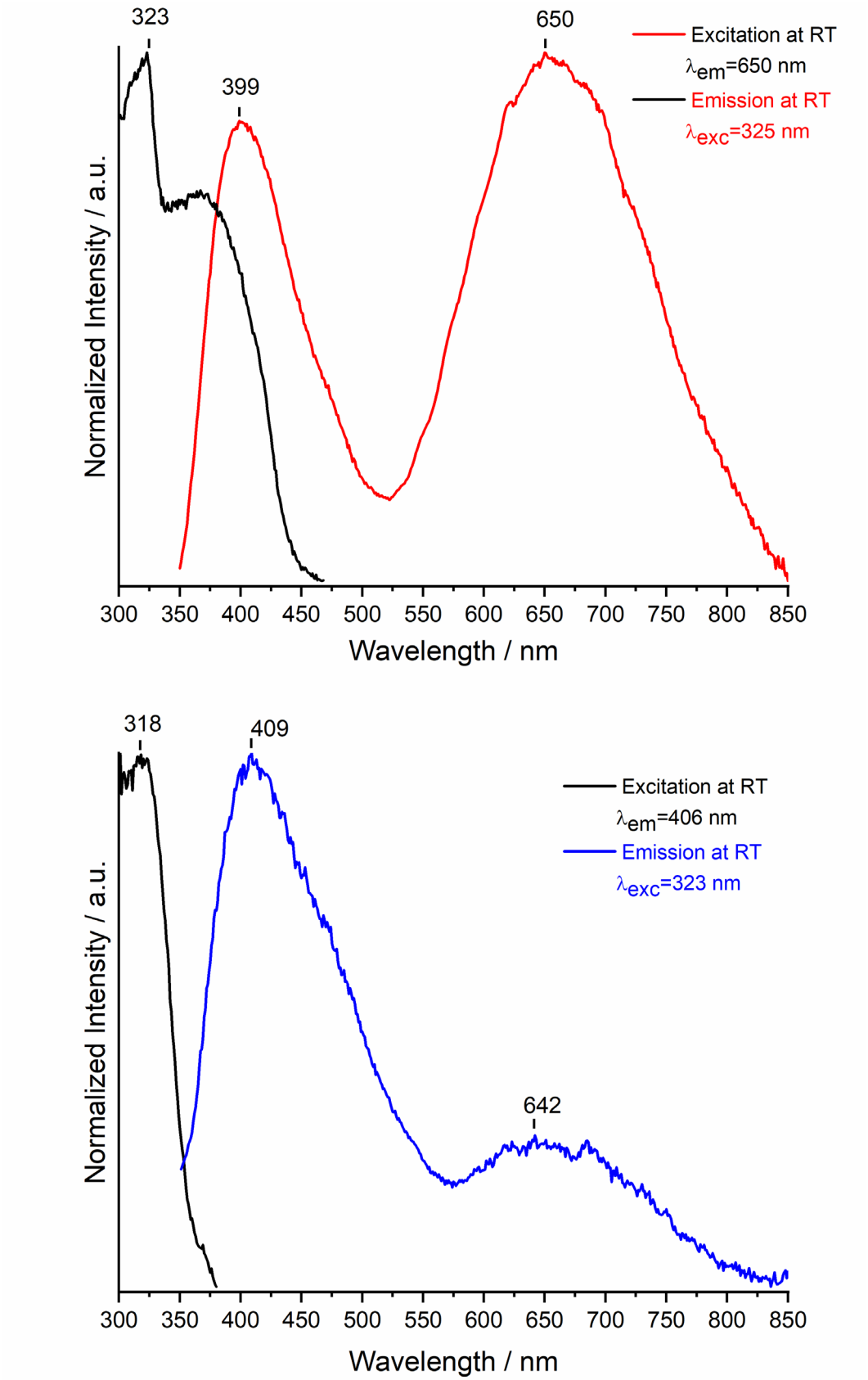

Figure S26. Normalized excitation and normalized emission spectra of $^{2}_{\infty}$[Ce(4-PyPz)$_3$(Py)] (**4-$^{2}_{\infty}$Ce**) at room temperature (top) and 77K (bottom). Wavelengths at which the spectra were recorded are reported in the legends.

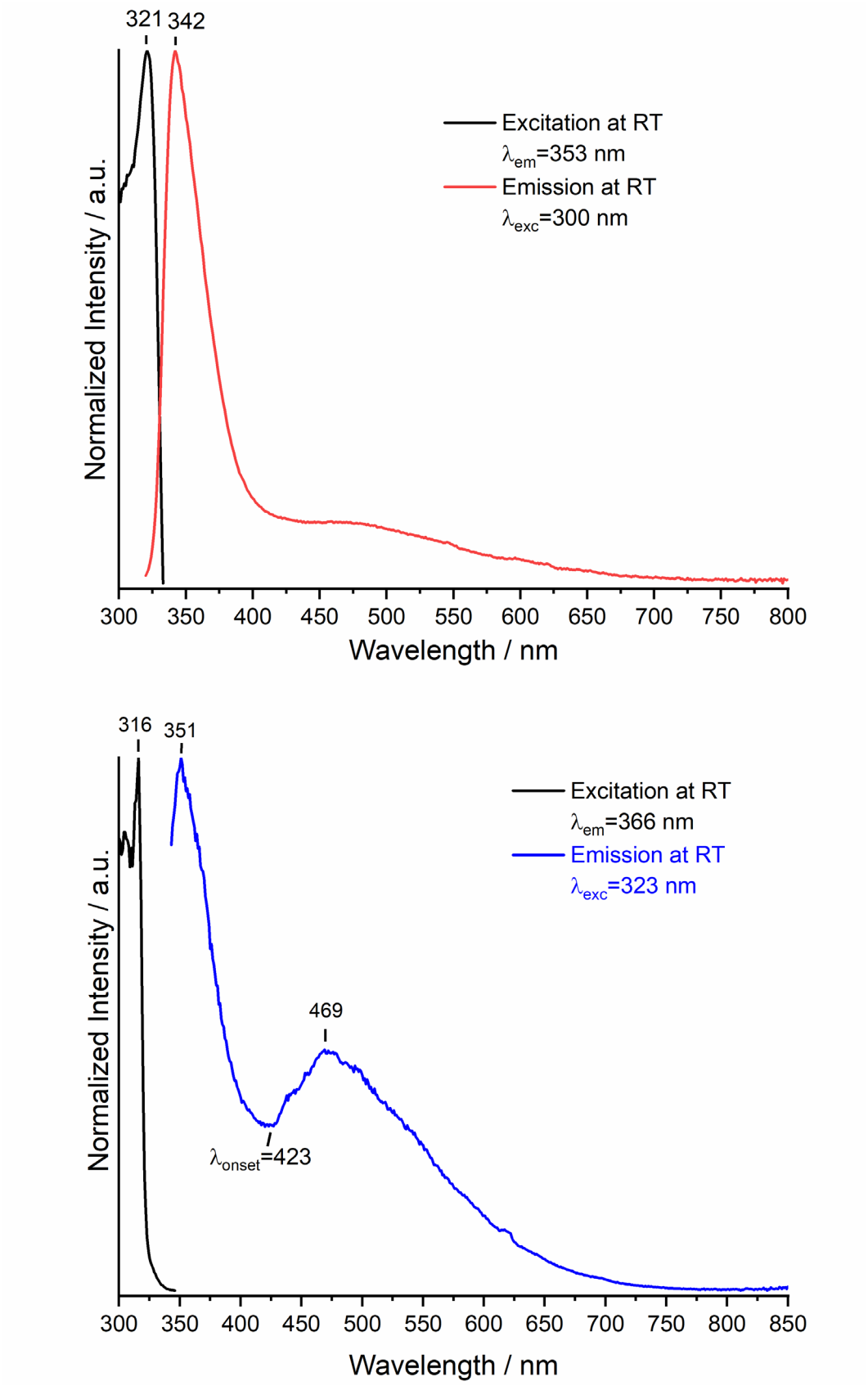

Figure S27. Normalized excitation and normalized emission spectra of $^{3}_{\infty}$[La(4-PyPz)$_3$] (**4-La**) at room temperature (top) and 77K (bottom). Wavelengths at which the spectra were recorded are reported in the legends.

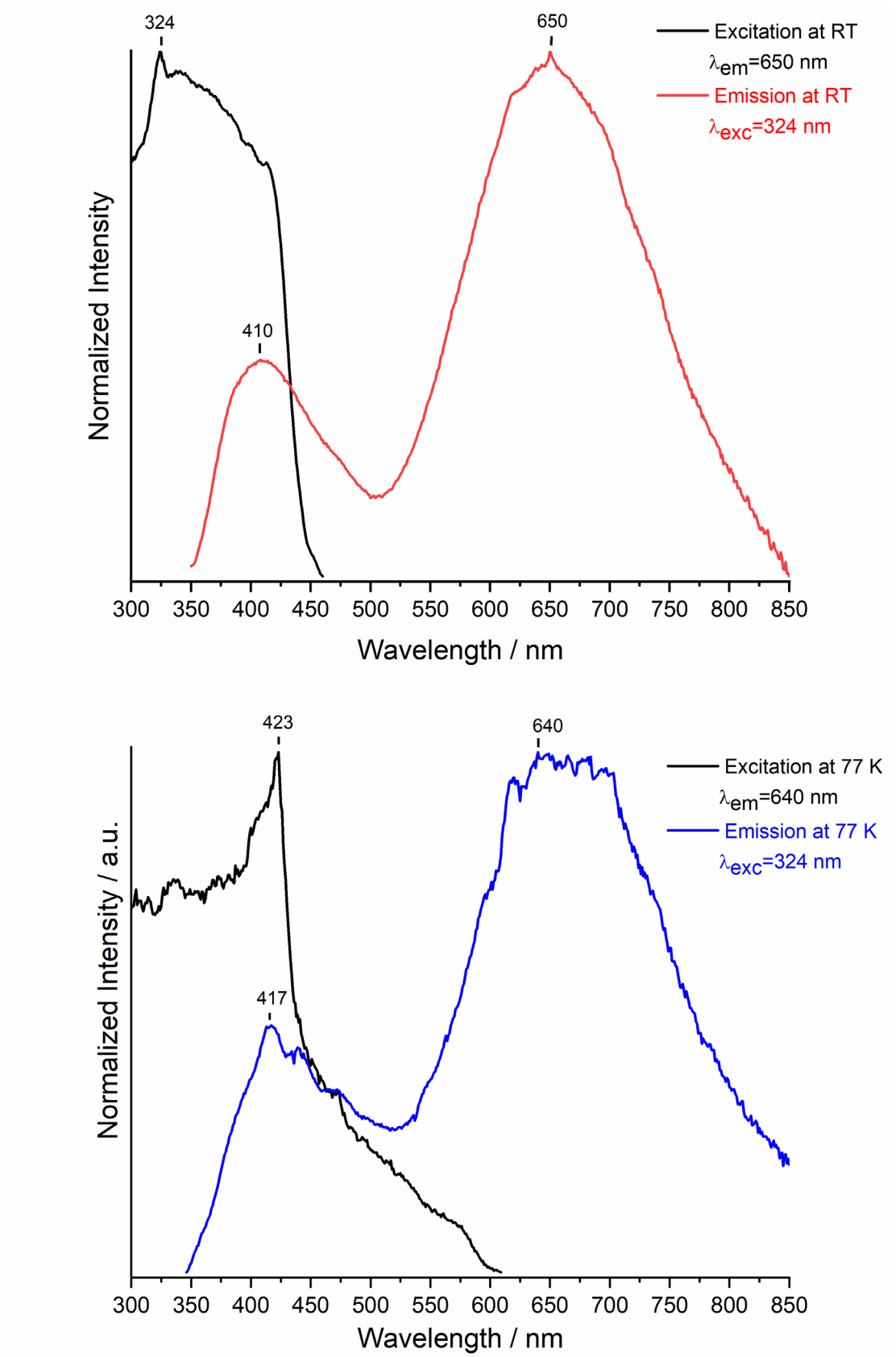

Figure S28. Normalized excitation and normalized emission spectra of $^{3}_{\infty}$[Ce(4-PyPz)$_3$] (**4-Ce**) at room temperature (top) and 77K (bottom). Wavelengths at which the spectra were recorded are reported in the legends.

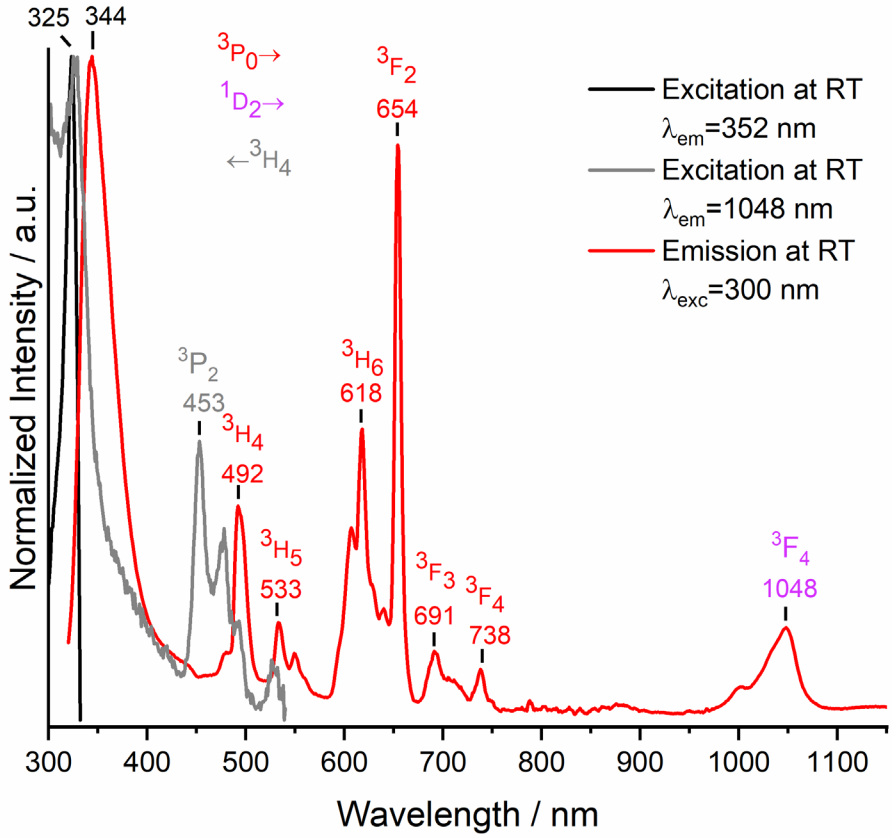

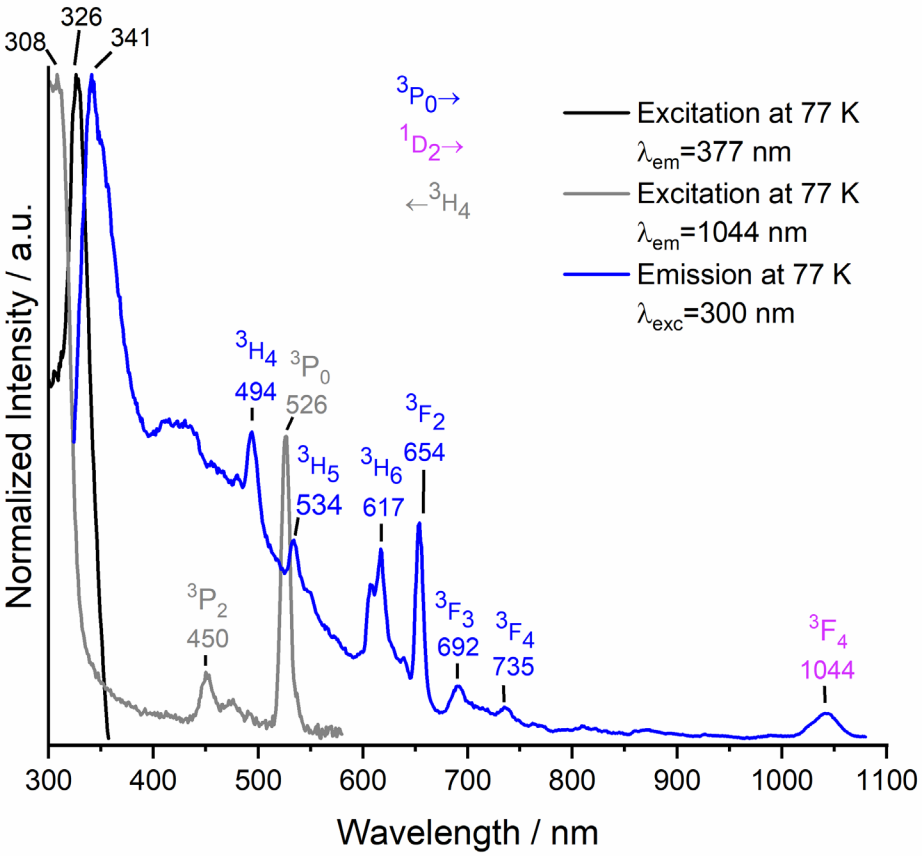

Figure S29. Normalized excitation and normalized emission spectra of $^3_\infty$[Pr(4-PyPz)$_3$] (**4-Pr**) at room temperature (top) and 77K (bottom). Visible and NIR range emission spectra were brought to the same intensity at 738 (at RT) and 735 (at 77 K) nm. Wavelengths at which the spectra were recorded are reported in the legends.

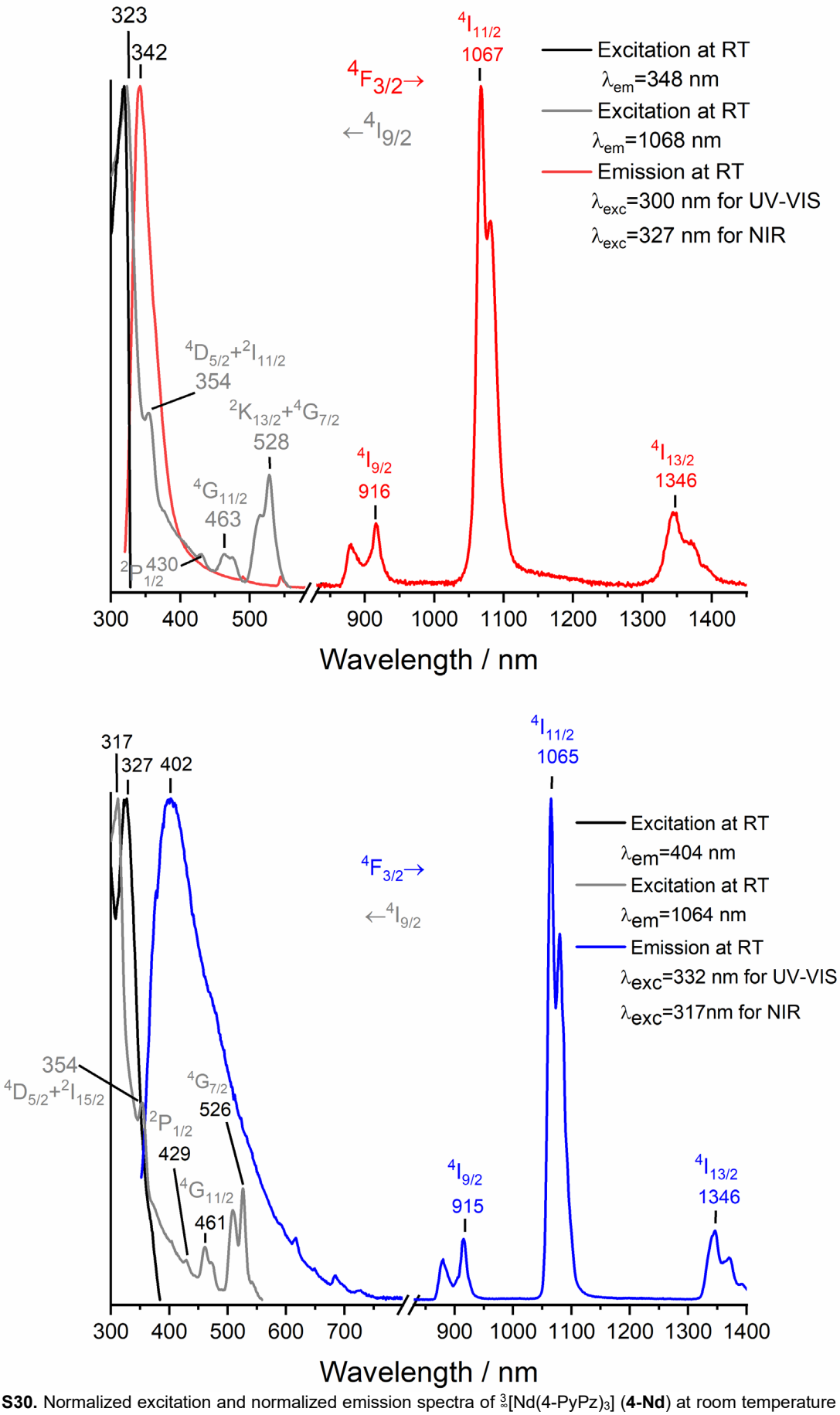

Figure S30. Normalized excitation and normalized emission spectra of $^3_{\infty}$[Nd(4-PyPz)$_3$] (**4-Nd**) at room temperature (top) and 77K (bottom). Wavelengths at which the spectra were recorded are reported in the legends.

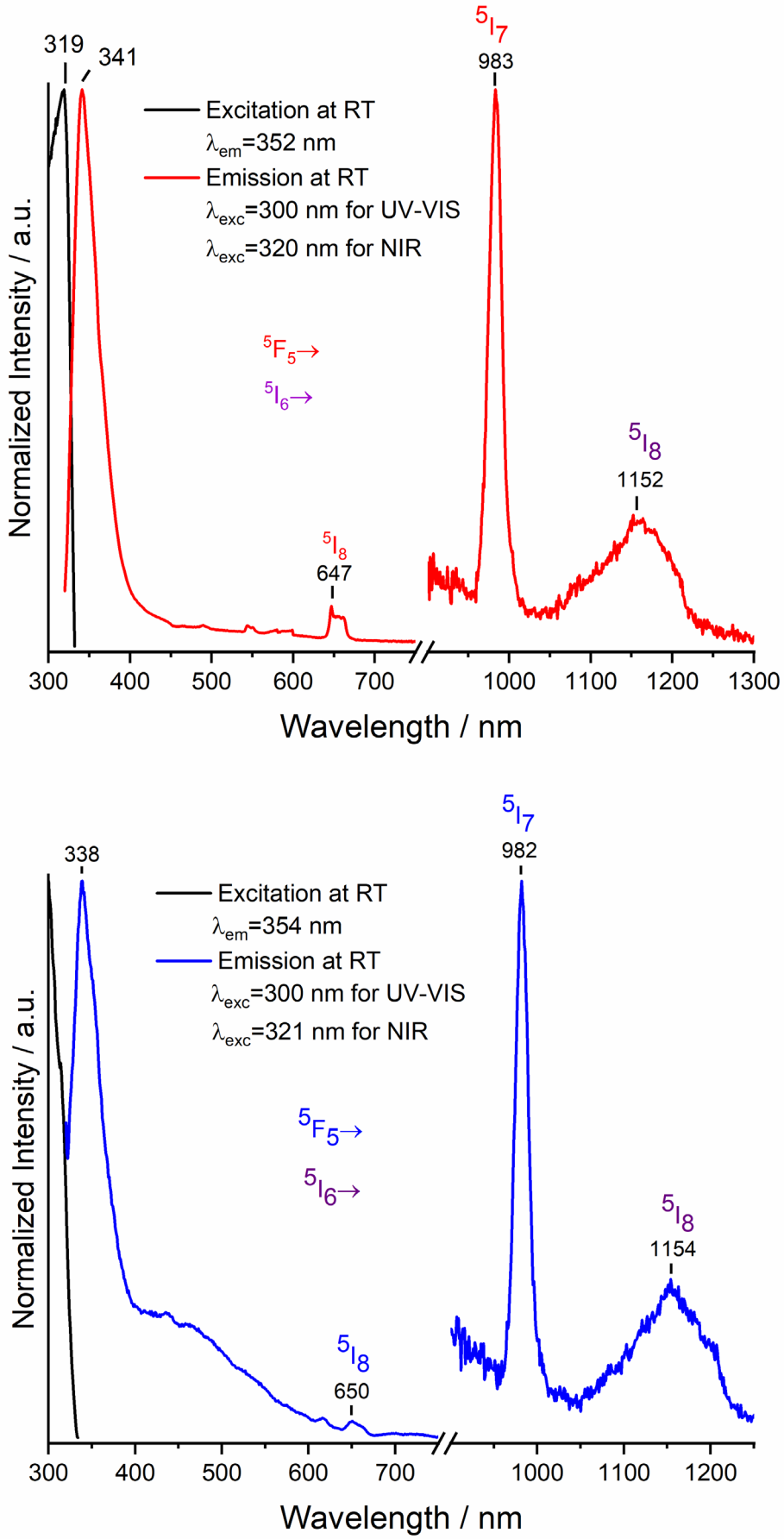

Figure S31. Normalized excitation and normalized emission spectra of $^3_\infty$[Ho(4-PyPz)$_3$] (**4-Ho**) at room temperature (top) and 77K (bottom). Wavelengths at which the spectra were recorded are reported in the legends.

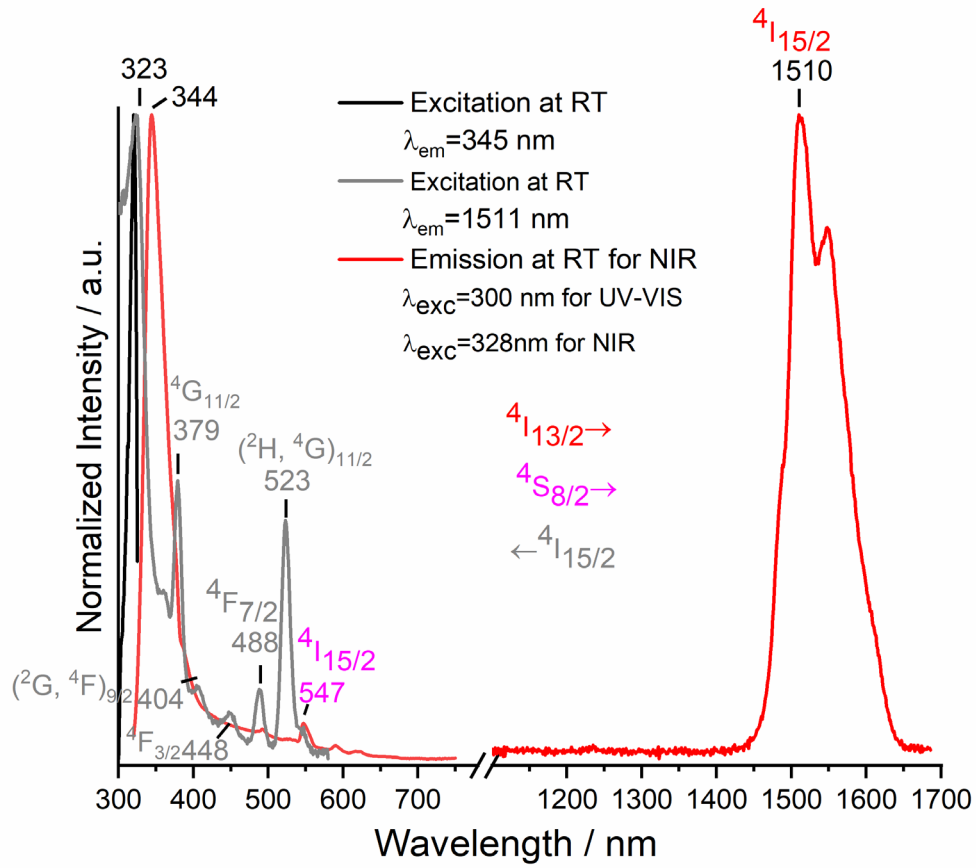

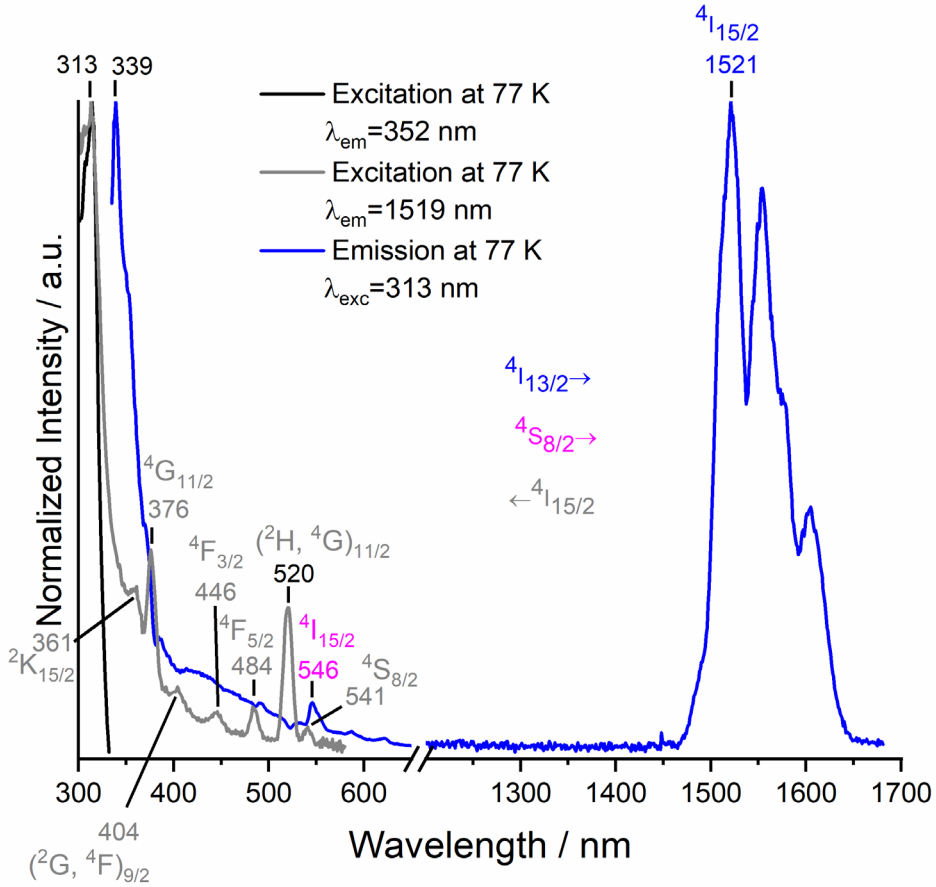

Figure S32. Normalized excitation and normalized emission spectra of $^{3}_{\infty}$[Er(4-PyPz)$_3$] (**4-Er**) at room temperature (top) and 77K (bottom). Wavelengths at which the spectra were recorded are reported in the legends.

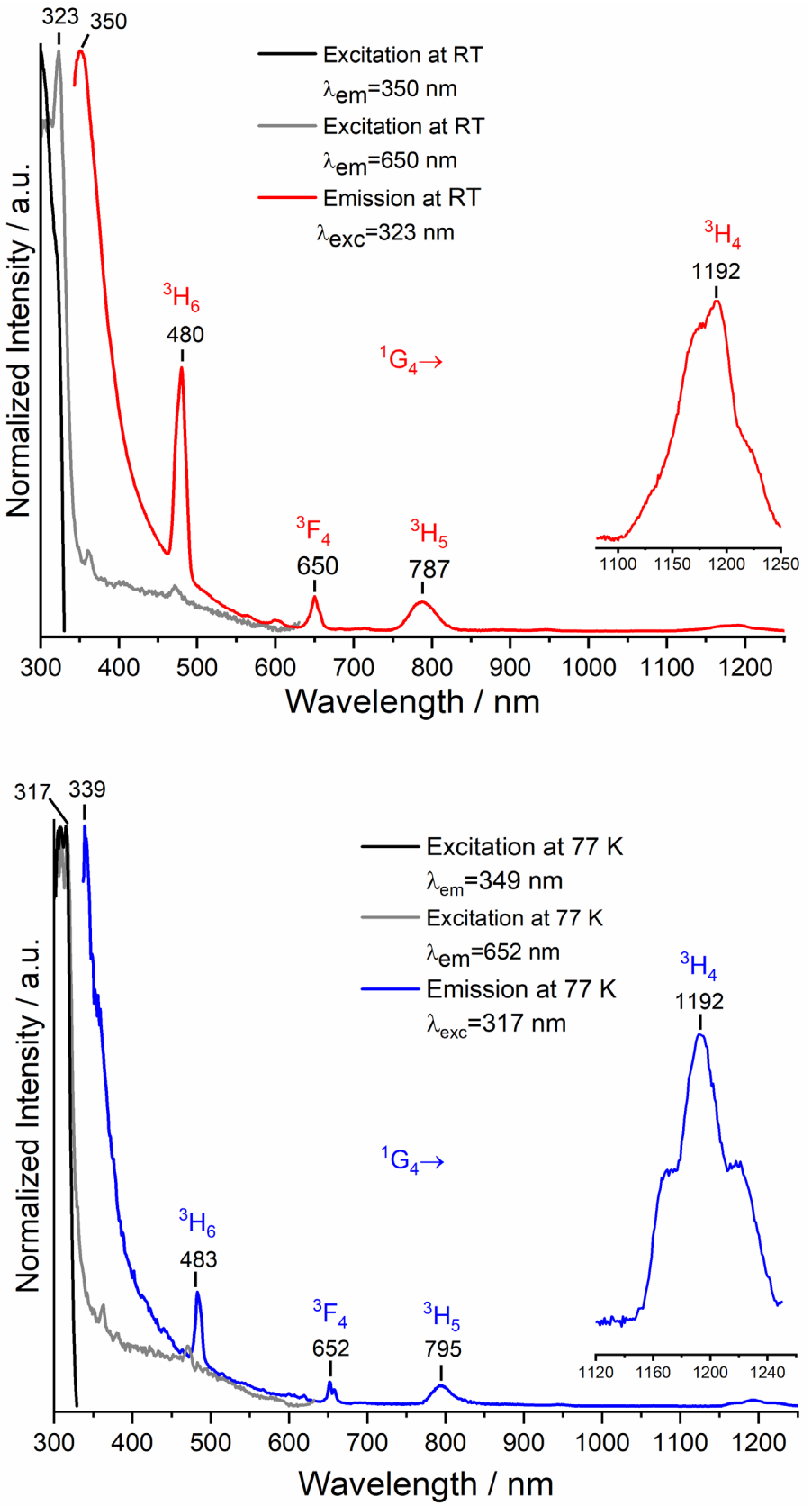

Figure S33. Normalized excitation and normalized emission spectra of $^{3}_{\infty}$[Tm(4-PyPz)$_3$] (**4-Tm**) at room temperature (top) and 77K (bottom). Visible and NIR range emission spectra were brought to the same intensity at 650 (at RT) and 652 (at 77 K) nm. Wavelengths at which the spectra were recorded are reported in the legends.

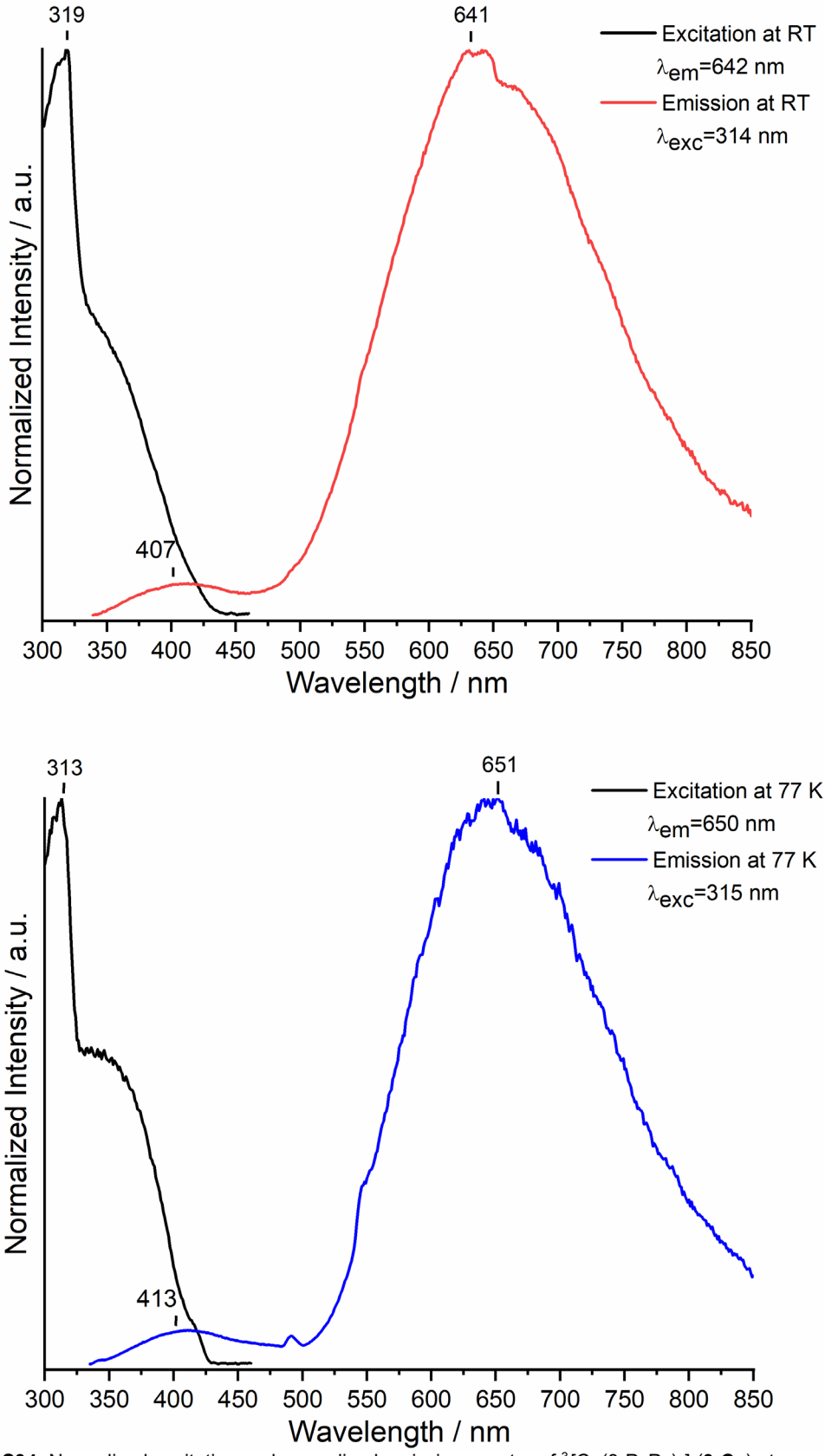

Figure S34. Normalized excitation and normalized emission spectra of $^{3}_{\infty}$[Ce(3-PyPz)$_3$] (**3-Ce**) at room temperature (top) and 77K (bottom). Wavelengths at which the spectra were recorded are reported in the legends.

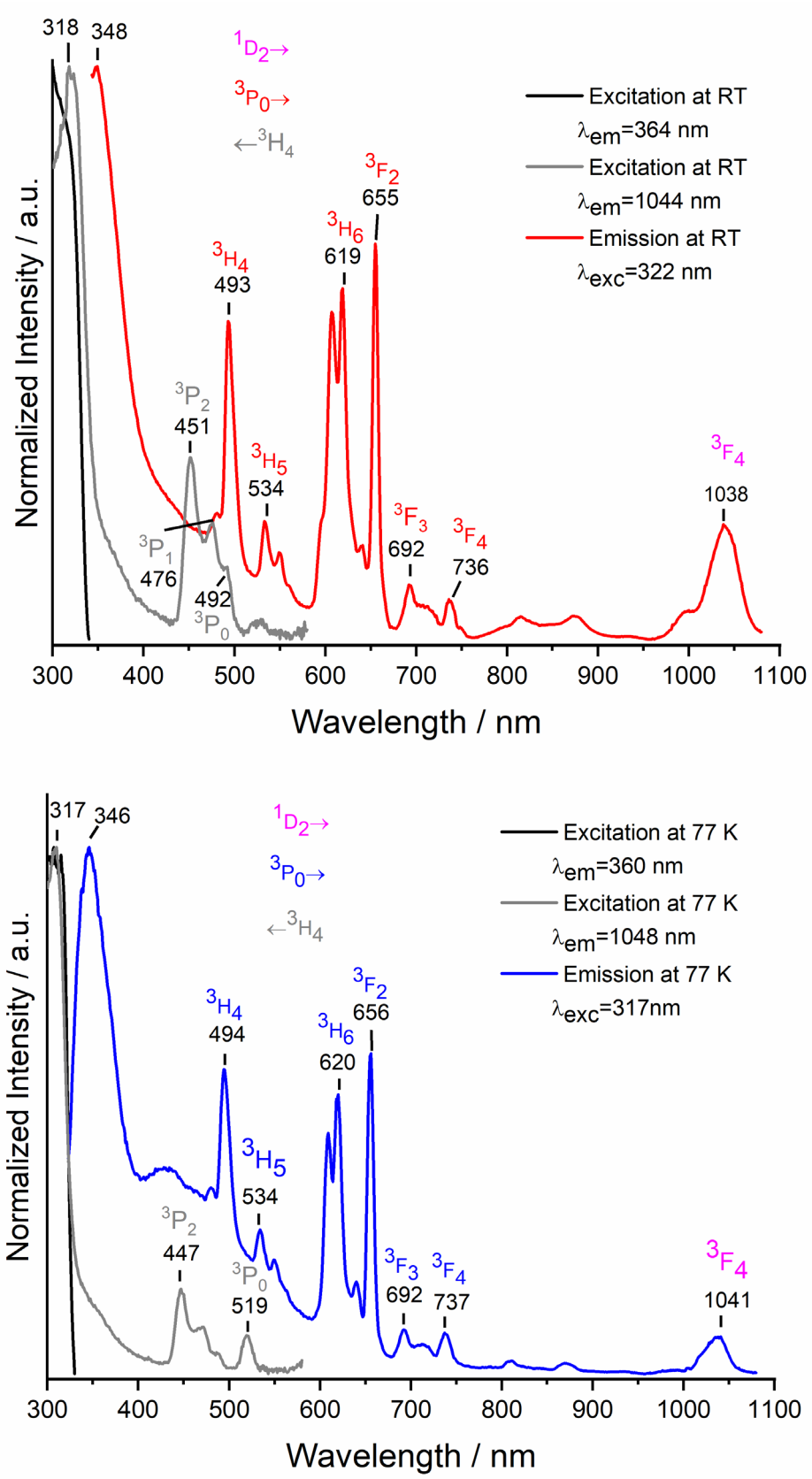

Figure S35. Normalized excitation and normalized emission spectra of $^3_\infty$[Pr(3-PyPz)$_3$] (**3-Pr**) at room temperature (top) and 77K (bottom). Visible and NIR range emission spectra were brought to the same intensity at 736 (at RT) and 737 (at 77 K) nm. Wavelengths at which the spectra were recorded are reported in the legends.

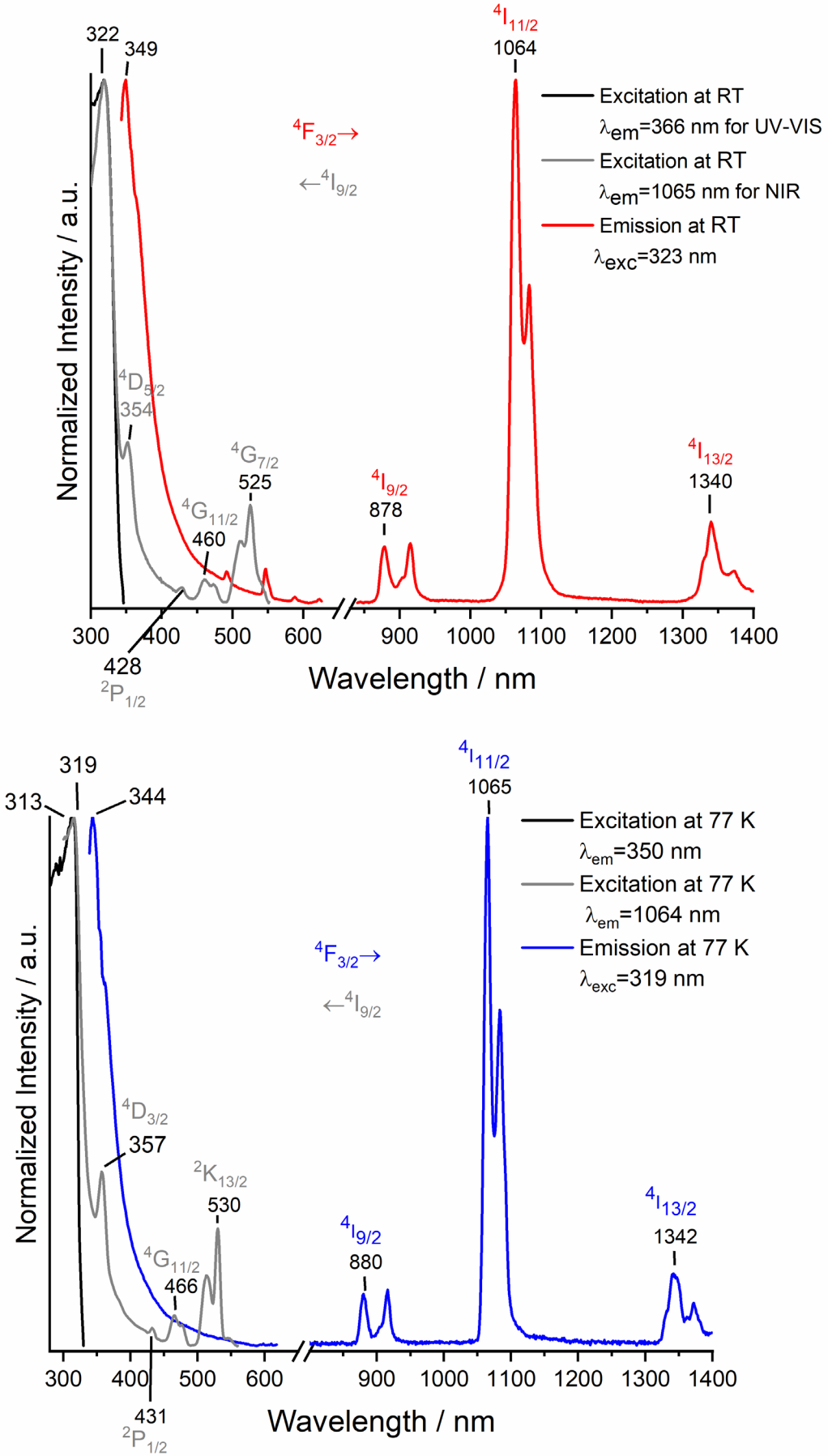

Figure S36. Normalized excitation and normalized emission spectra of $^3_\infty$[Nd(3-PyPz)$_3$] (**3-Nd**) at room temperature (top) and 77K (bottom). Wavelengths at which the spectra were recorded are reported in the legends.

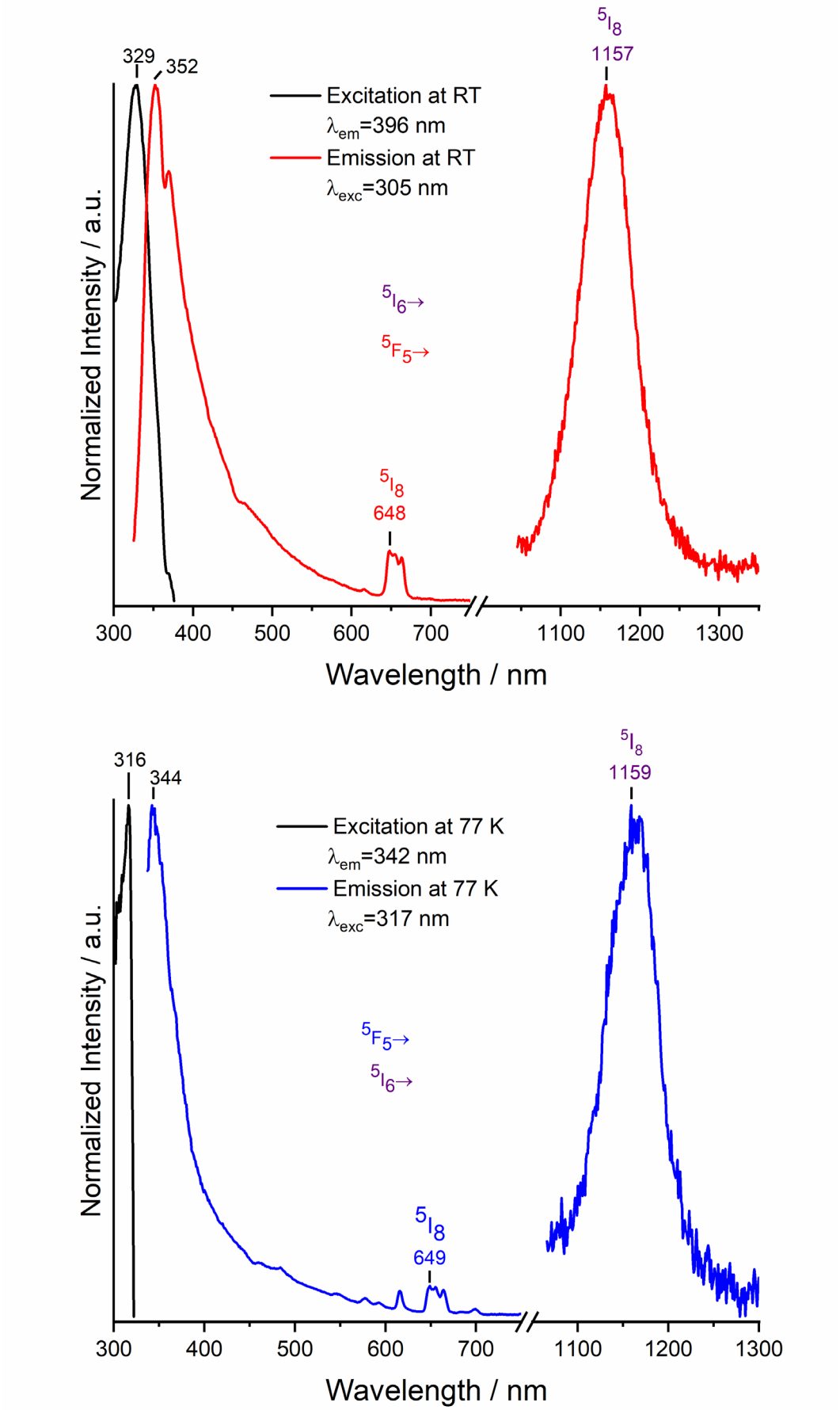

Figure S37. Normalized excitation and normalized emission spectra of $^{3}_{\infty}$[Ho(3-PyPz)$_3$] (**3-Ho**) at room temperature (top) and 77K (bottom). Wavelengths at which the spectra were recorded are reported in the legends.

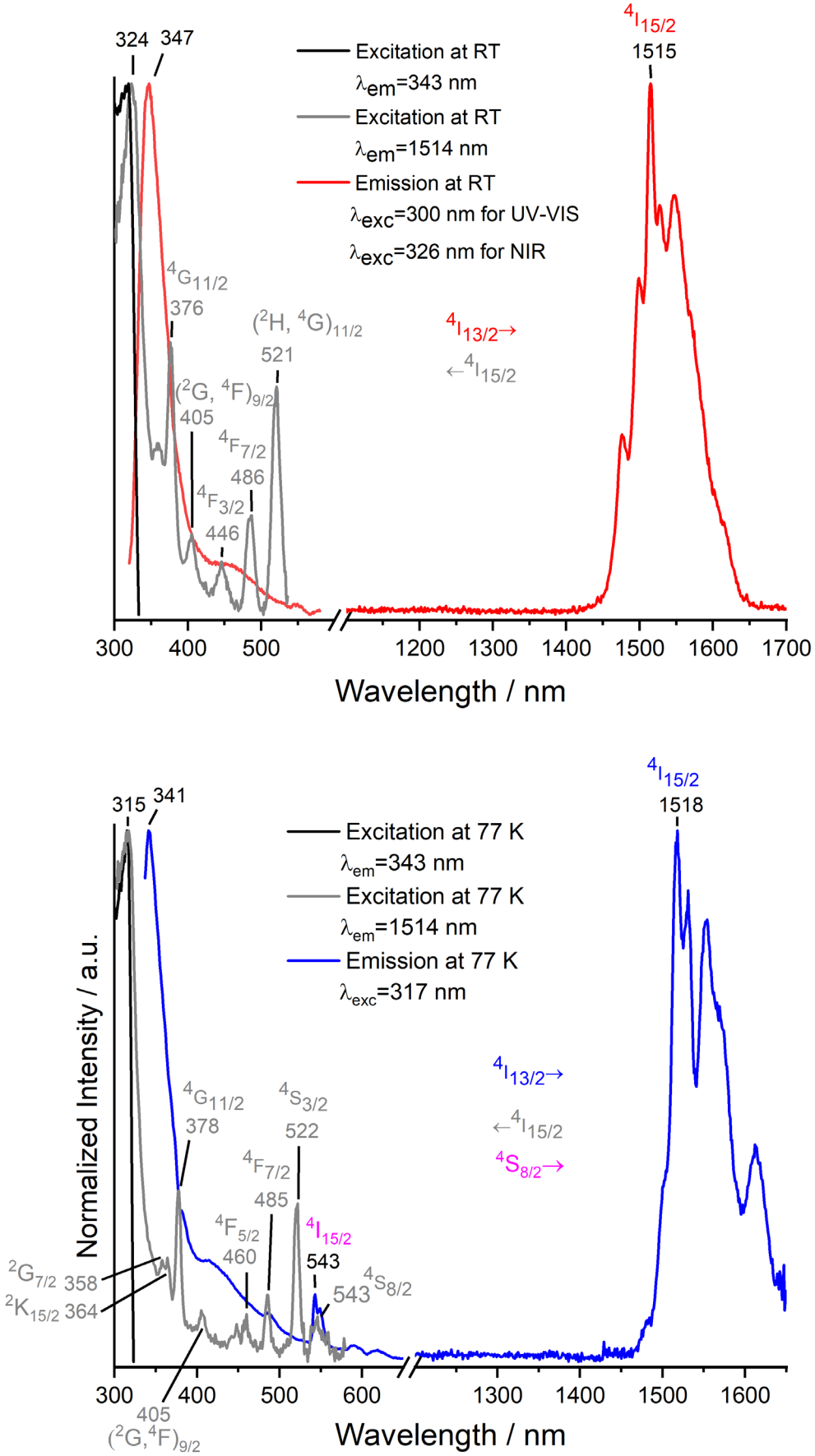

Figure S38. Normalized excitation and normalized emission spectra of $^{3}_{\infty}$[Er(3-PyPz)$_3$] (**3-Er**) at room temperature (top) and 77K (bottom). Wavelengths at which the spectra were recorded are reported in the legends.

Table S14. Photophysical data of $^{2}_{\infty}$[Eu(4-PyPz)$_2$(Py)$_2$] (**4-Eu^{2+}**), $^{2}_{\infty}$[Ce(4-PyPz)$_3$(Py)] (**4-$^{2}_{\infty}$Ce**), $^{3}_{\infty}$[Ln(4-PyPz)$_3$], (**4**, Ln = La, Ce, Pr, Nd, Ho, Er, Tm) and $^{3}_{\infty}$[Ln(3-PyPz)$_3$], (**3**, Ln = Ce, Pr, Nd, Ho, Er) in the solid state at room temperature and 77 K.

ID	$\tau_{(RT)}$[a]	$\lambda_{ex}/\lambda_{em}$ [nm][b]	$\tau_{(77\ K)}$[c]	$\lambda_{ex}/\lambda_{em}$ [nm][d]
4-Eu^{2+}	1.34(3) ns	287/385	2.18(5) ns	287/377
4-$^{2}_{\infty}$Ce	1.08(2) ns	287/650	1.18(3) ns	287/643
4-Ce	1.16(2) ns	287/650	1.06(5) ns	287/640
3-Ce	1.26(2) ns	287/641	1.20(3) ns	287/650
4-La	1.079(5) ns	287/342	1.738(9) ns	351/287
			<2 µs	316/469
4-Pr	0.96(2) ns	287/344	1.23(5) ns	287/341
3-Pr	0.99(2) ns	287/348	1.20(2) ns	287/346
4-Nd	0.93(2) ns	287/342	3.04(9) ns	287/402
3-Nd	0.99(2) ns	287/349	1.30(2) ns	287/344
4-Ho	0.97(2) ns	287/341	1.34(4) ns	287/338
3-Ho	1.00(2) ns	287/352	1.19(2) ns	287/344
4-Er	0.98(1) ns	287/344	1.16(5) ns	287/339
3-Er	1.02(1) ns	287/347	1.19(4) ns	287/341
4-Tm	1.04(1) ns	287/350	1.15(3) ns	287/349

[a] Emission lifetime determined at RT. [b] Excitation and emission wavelengths for emission lifetime at RT. [c] Emission lifetime determined at 77 K. [d] Excitation and emission wavelengths for emission lifetime at 77 K.

IR Spectroscopy

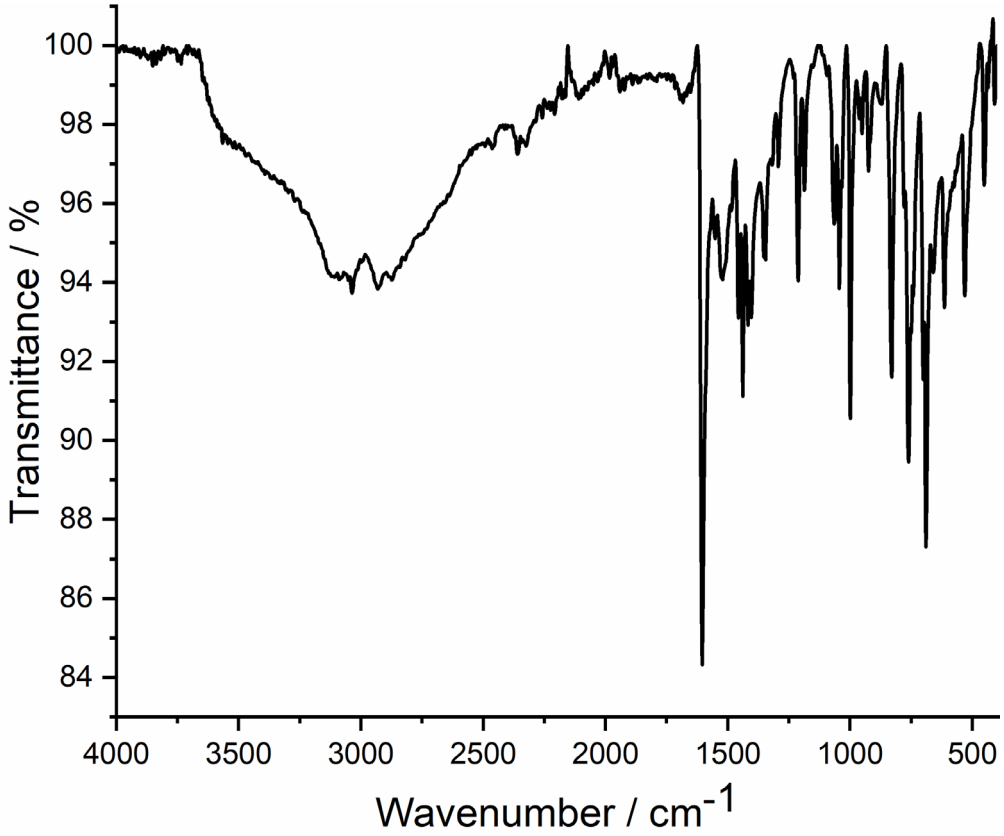

Figure S39. The infrared spectrum (ATR) of coordination polymer $^{2}_{\infty}$[Eu(4-PyPz)$_3$(Py)$_2$] (**4-Eu^{2+}**).

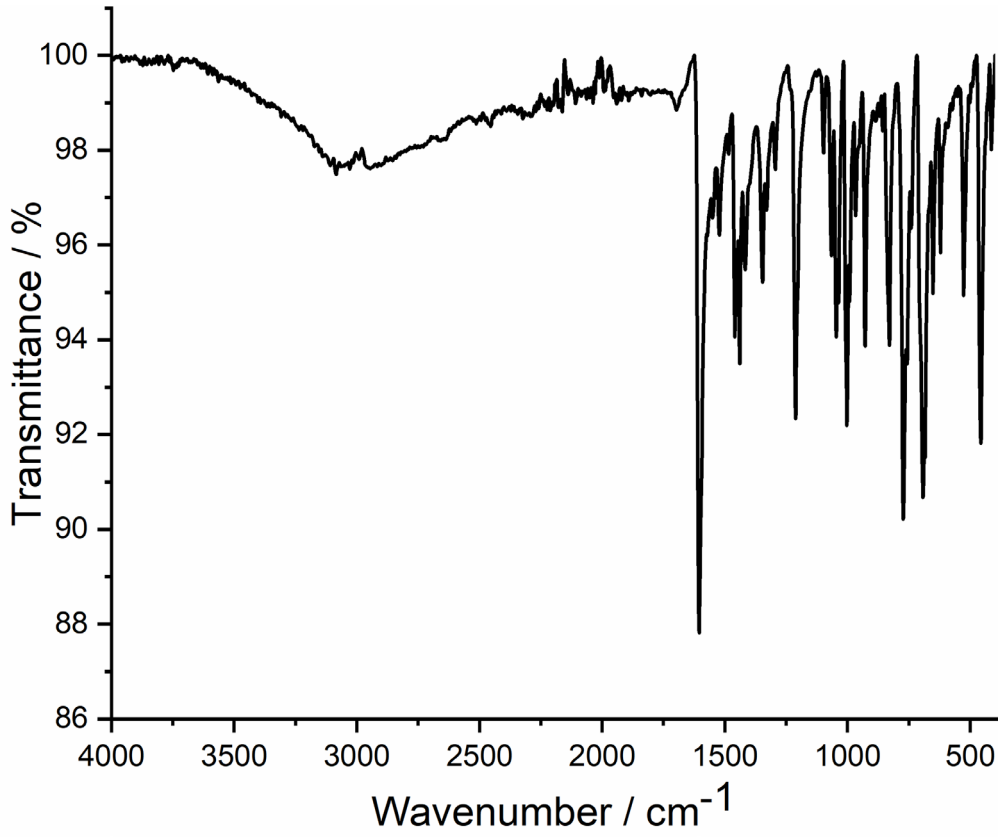

Figure S40. The infrared spectrum (ATR) of coordination polymer $^{2}_{\infty}$[Ce(4-PyPz)$_3$(Py)] (**4-$^{2}_{\infty}$Ce**).

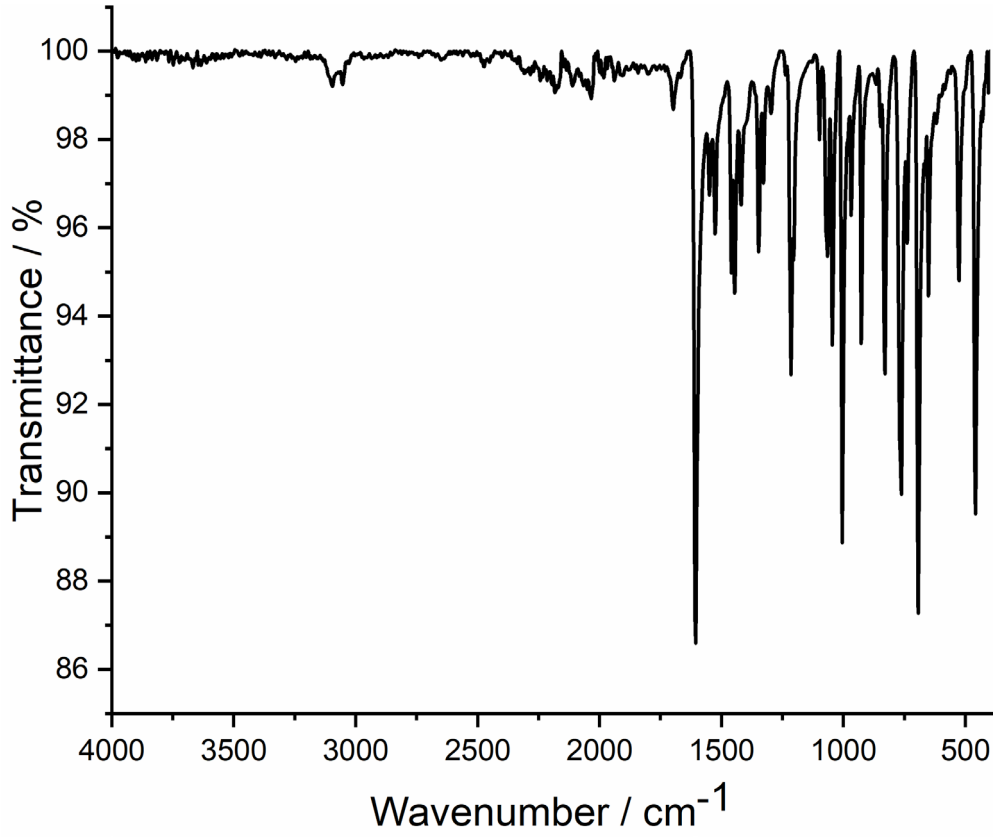

Figure S41. The infrared spectrum (ATR) of coordination polymer of $^{3}_{\infty}$[La(4-PyPz)$_3$] (**4-La**).

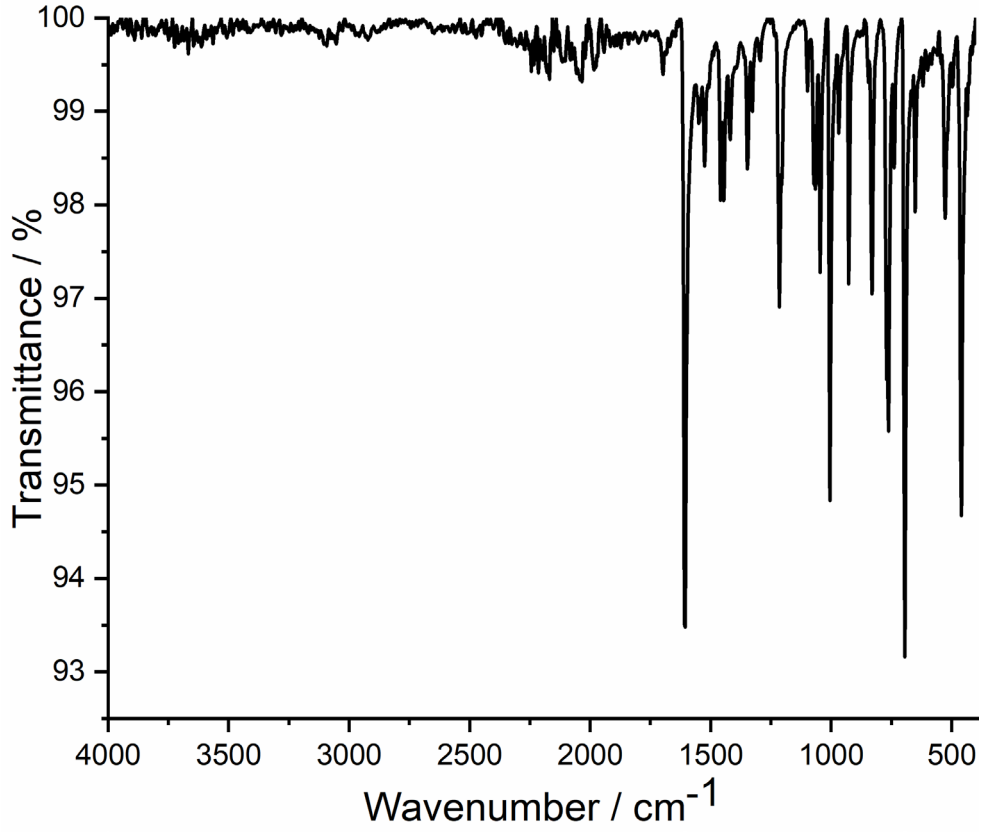

Figure S42. The infrared spectrum (ATR) of coordination polymer of $^{3}_{\infty}$[Ce(4-PyPz)$_3$] (**4-Ce**).

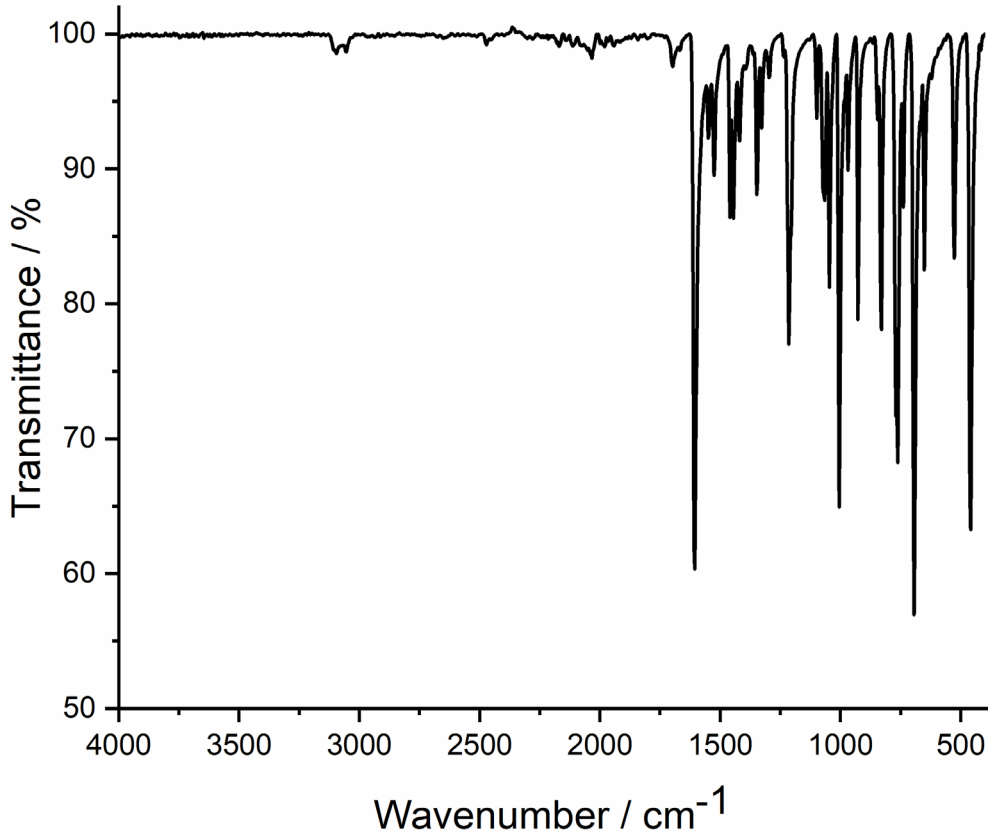

Figure S43. The infrared spectrum (ATR) of coordination polymer of $^{3}_{\infty}$[Pr(4-PyPz)$_3$] (**4-Pr**).

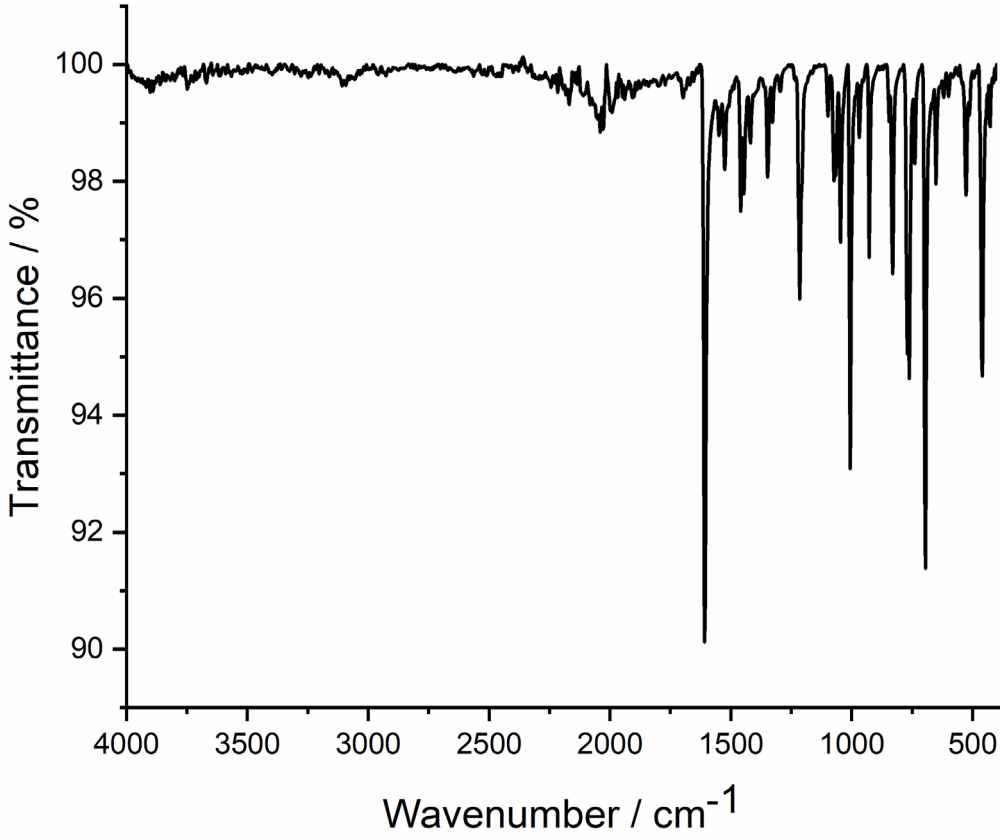

Figure S44. The infrared spectrum (ATR) of coordination polymer of $^{3}_{\infty}$[Nd(4-PyPz)$_3$] (**4-Nd**).

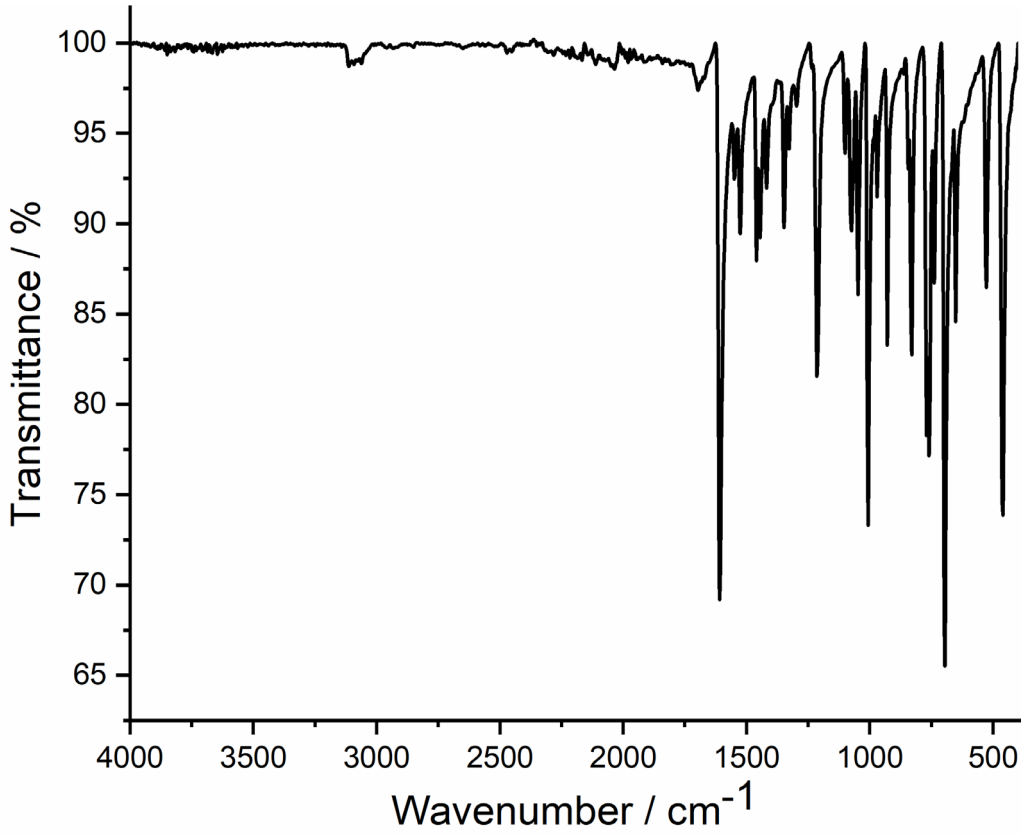

Figure S45. The infrared spectrum (ATR) of coordination polymer of $^{3}_{\infty}$[Ho(4-PyPz)$_3$] (**4-Ho**).

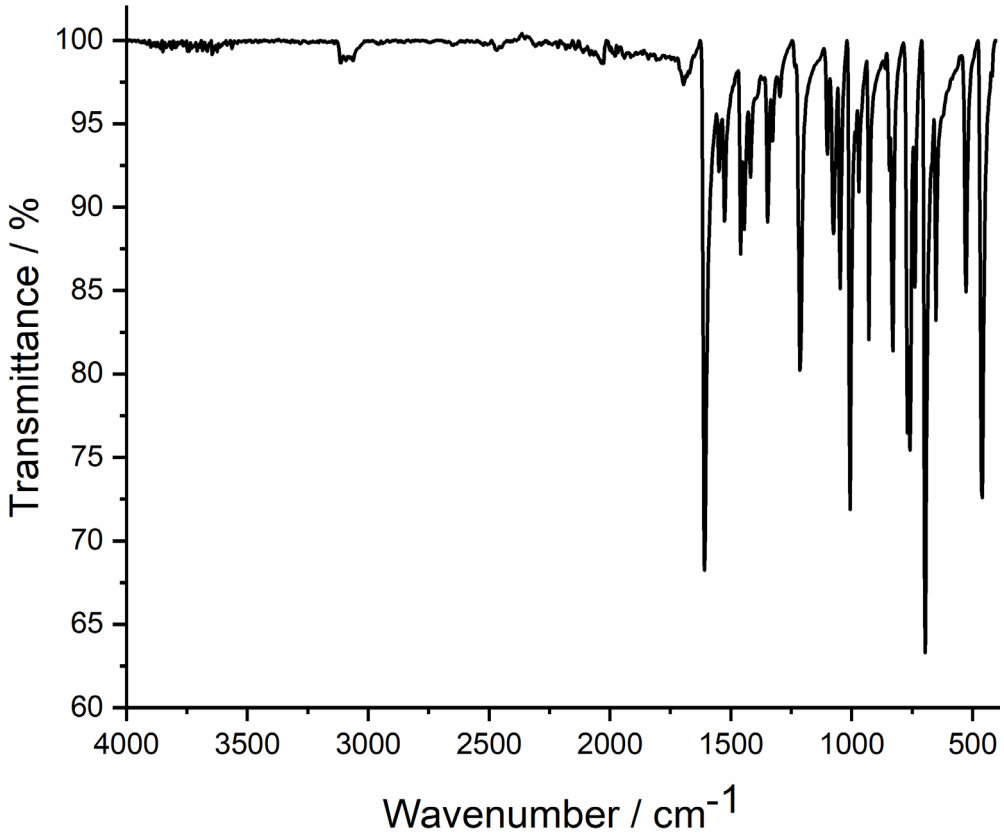

Figure S46. The infrared spectrum (ATR) of coordination polymer of $^{3}_{\infty}$[Er(4-PyPz)$_3$] (**4-Er**).

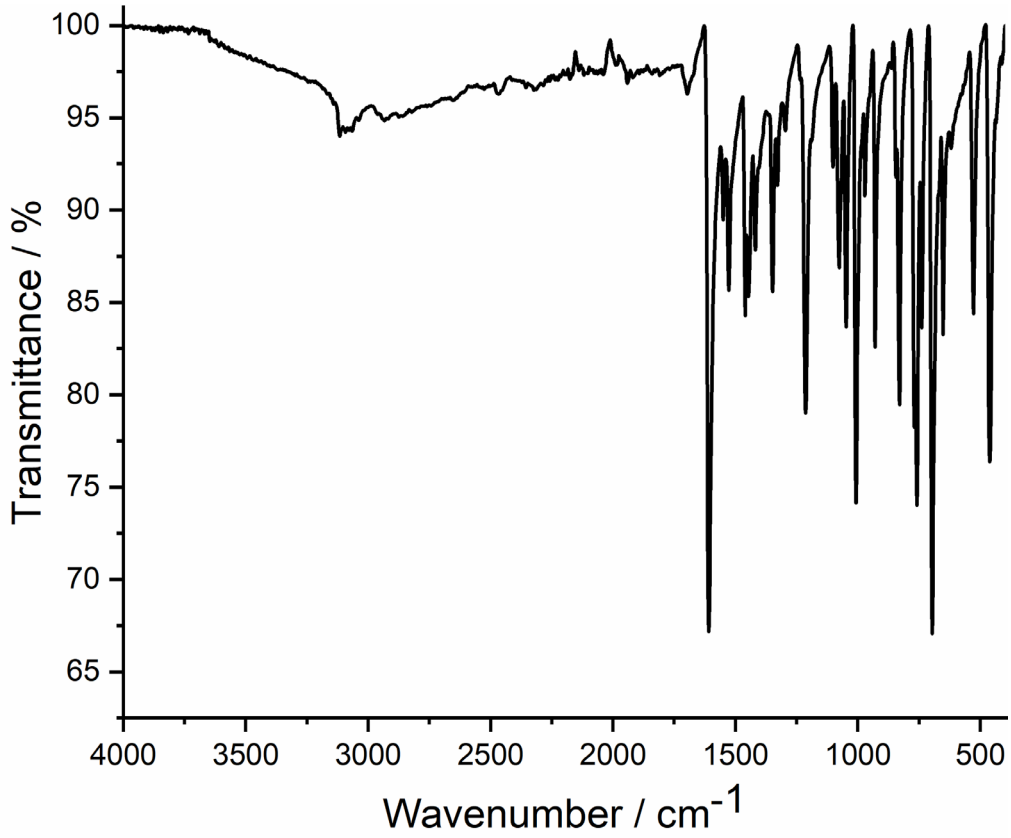

Figure S47. The infrared spectrum (ATR) of coordination polymer $^{3}_{\infty}$[Tm(4-PyPz)$_3$] (**4-Tm**).

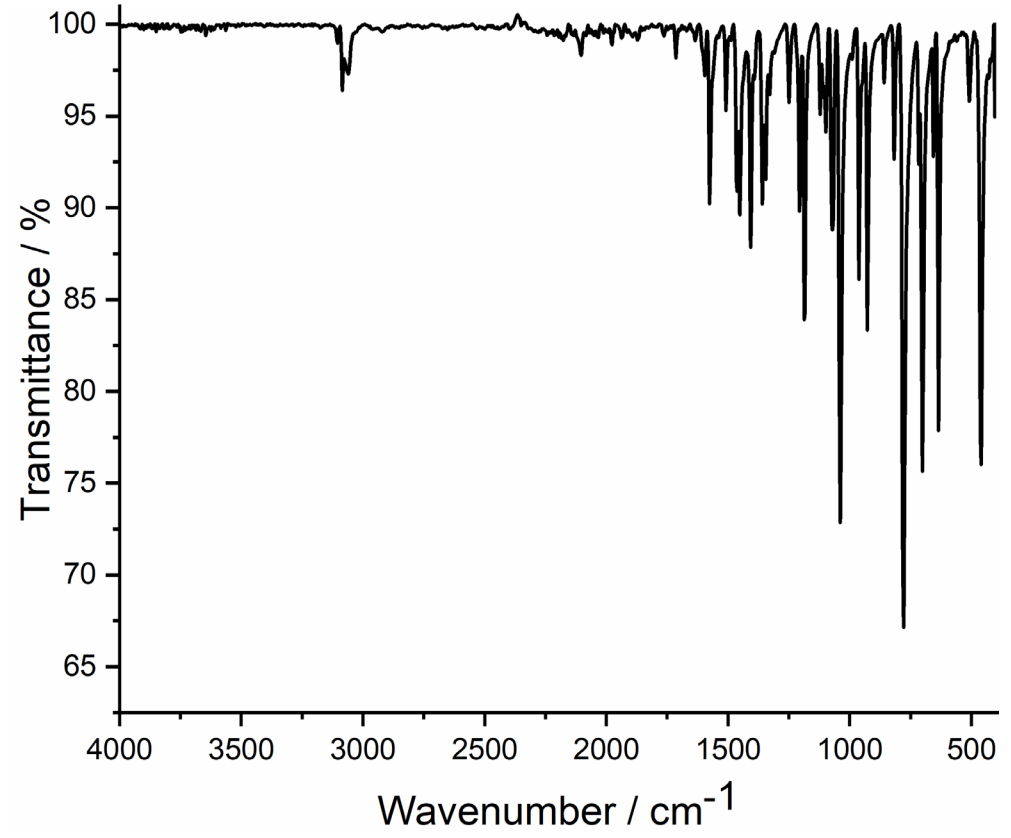

Figure S48. The infrared spectrum (ATR) of coordination polymer of $^{3}_{\infty}$[Ce(3-PyPz)$_3$] (**3-Ce**).

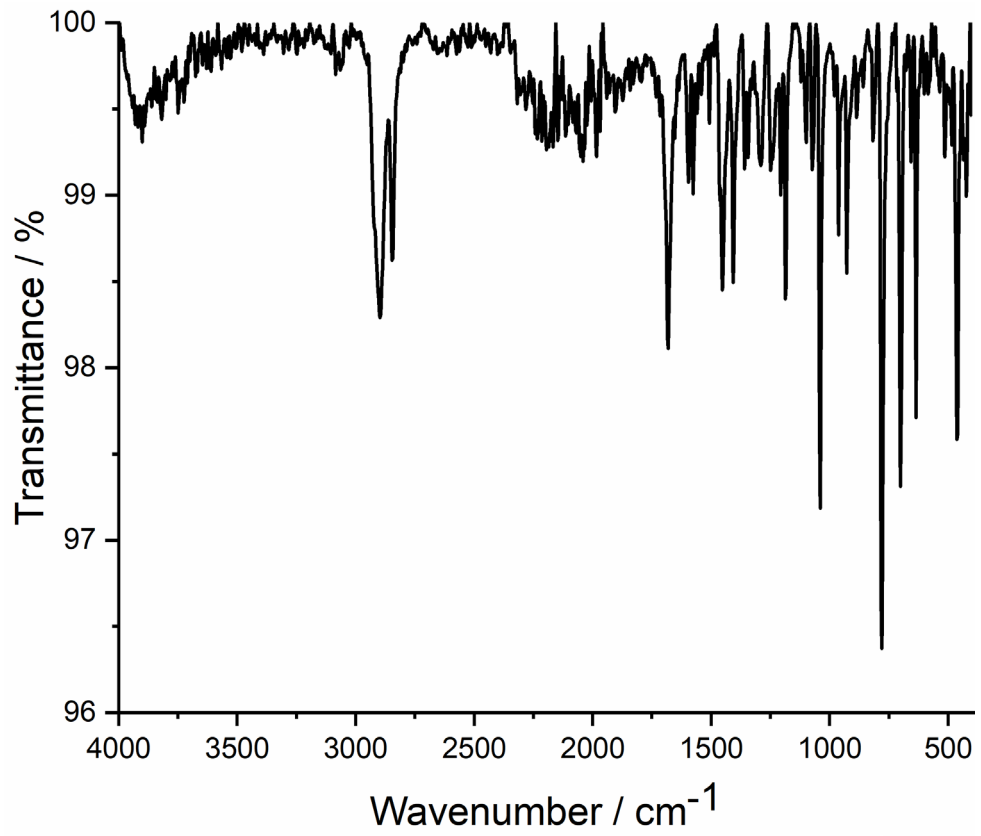

Figure S49. The infrared spectrum (ATR) of coordination polymer of $^{3}_{\infty}$[Pr(3-PyPz)$_3$] (**3-Pr**).

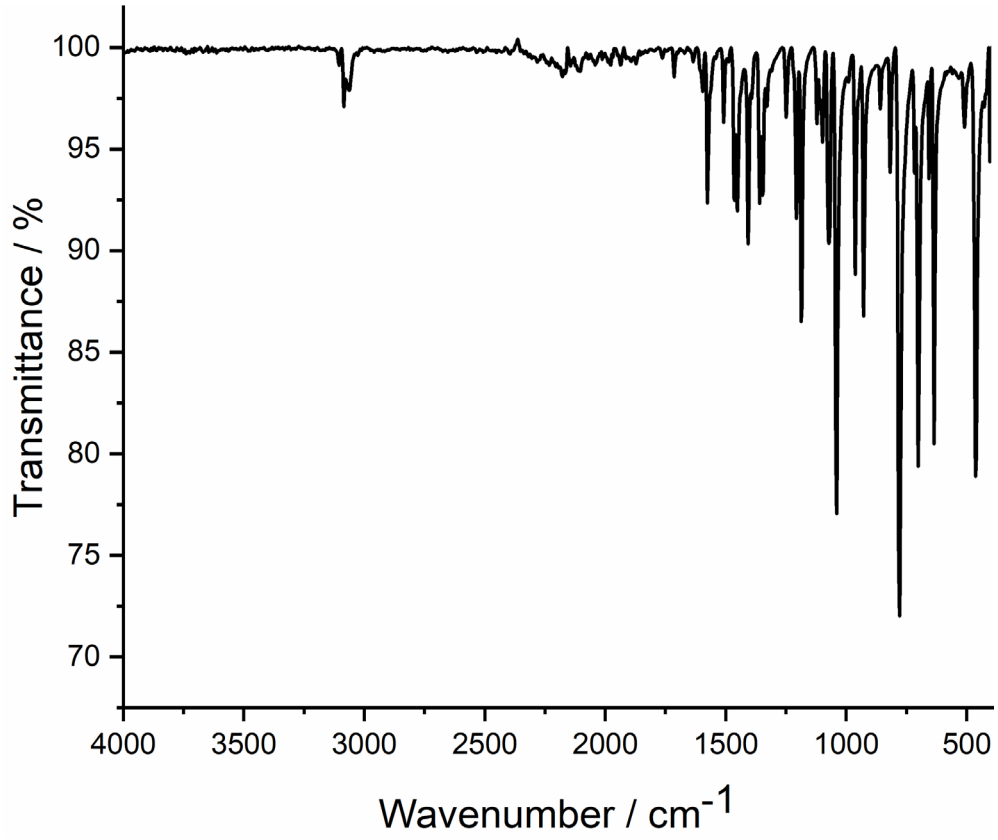

Figure S50. The infrared spectrum (ATR) of coordination polymer of $^{3}_{\infty}$[Nd(3-PyPz)$_3$] (**3-Nd**).

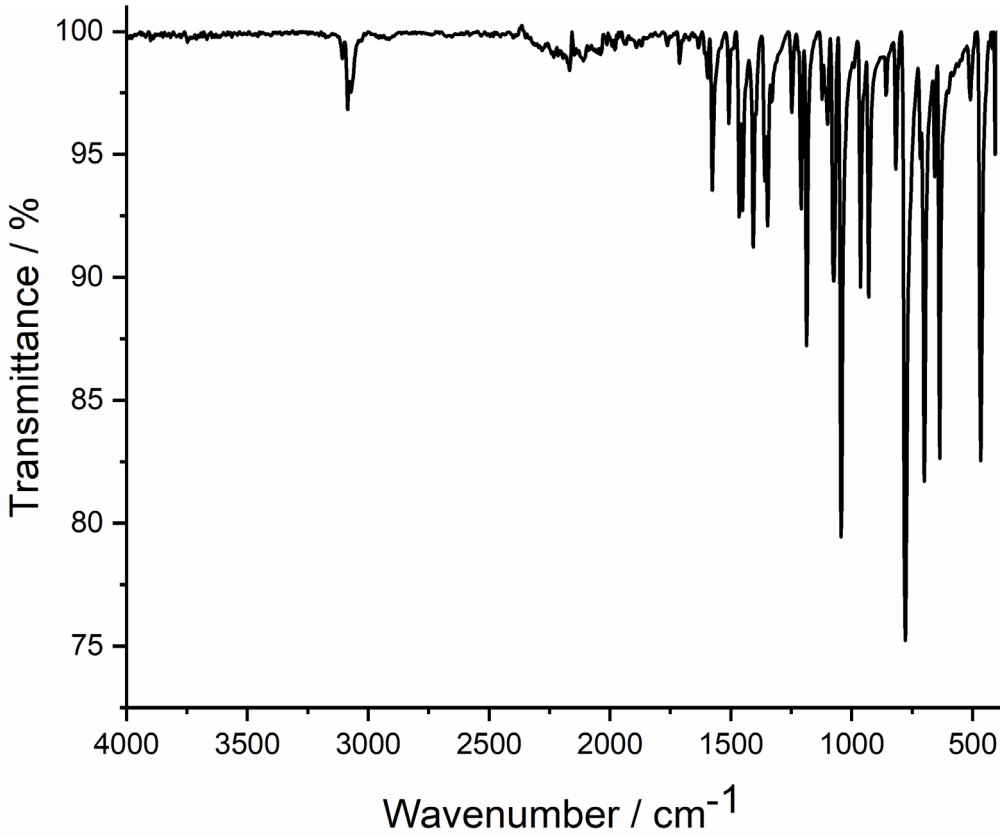

Figure S51. The infrared spectrum (ATR) of coordination polymer of $^{3}_{\infty}$[Ho(3-PyPz)$_3$] (**3-Ho**).

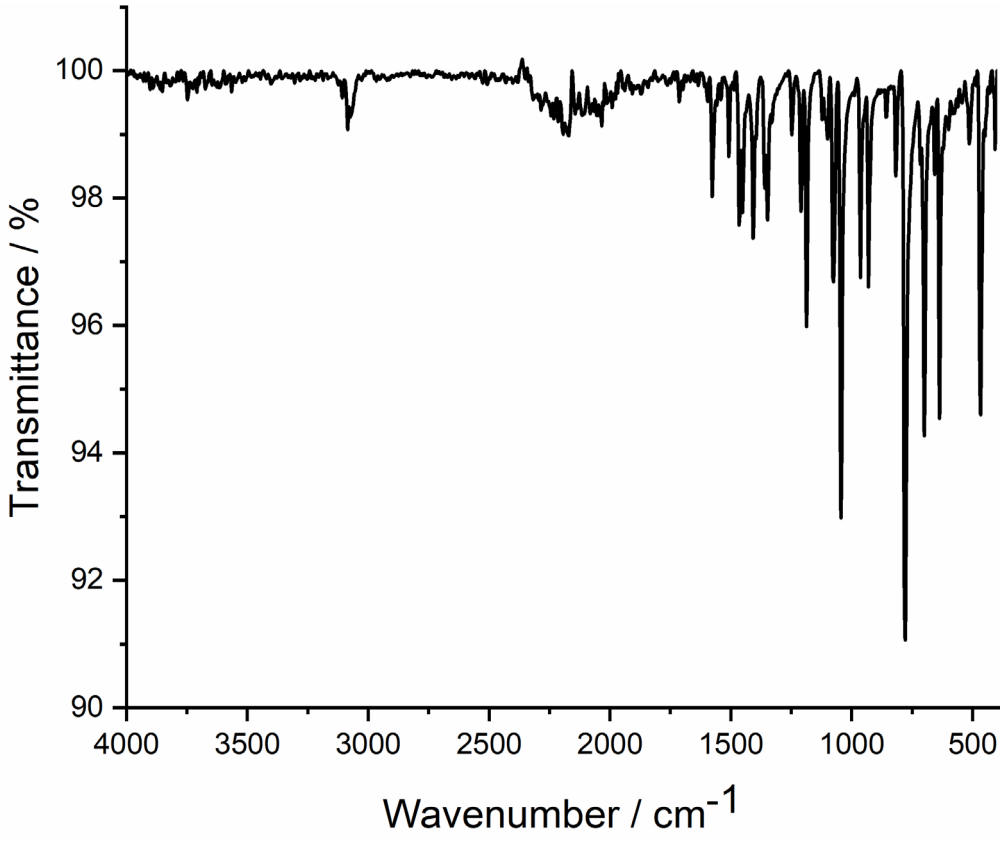

Figure S52. The infrared spectrum (ATR) of coordination polymer of $^{3}_{\infty}$[Er(3-PyPz)$_3$] (**3-Er**).

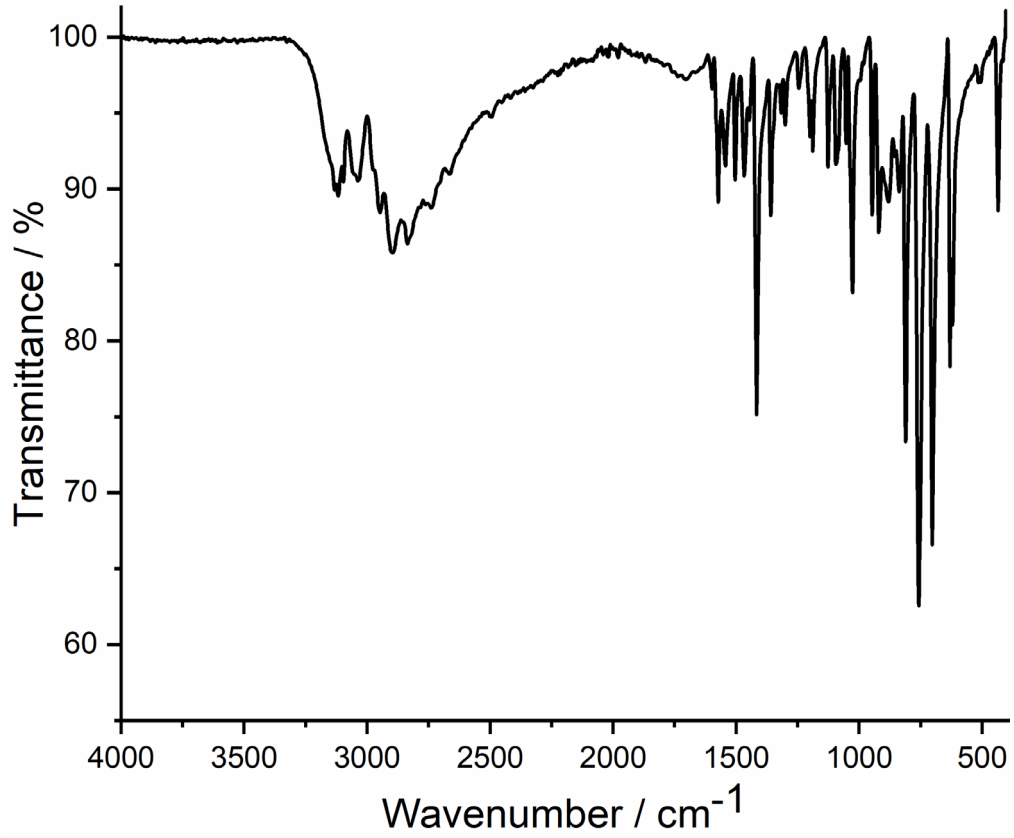

Figure S53. The infrared spectrum (ATR) of 3-PyPzH.

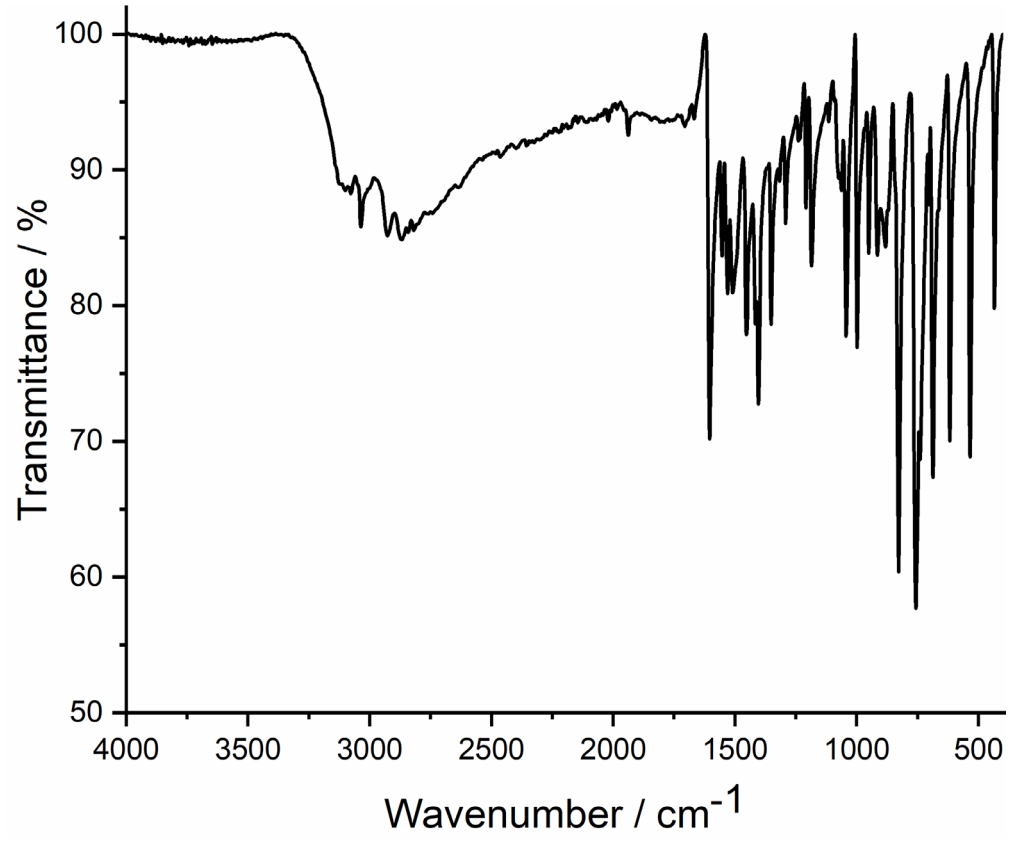

Figure S54. The infrared spectrum (ATR) of 4-PyPzH.